# Advancing the Extraction of Mechanical Properties from Biaxial Data

by

Carl Azzi

A thesis
presented to the University of Waterloo
in fulfillment of the
thesis requirement for the degree of
Master of Applied Science
in
Systems Design Engineering

Waterloo, Ontario, Canada, 2023

© Carl Azzi 2023

## Author's Declaration

I hereby declare that I am the sole author of this thesis. This is a true copy of the thesis, including any required final revisions, as accepted by my examiners.

I understand that my thesis may be made electronically available to the public.

**Abstract**

Mechanical characterization is vital to understand soft tissue behaviour in health and pathology. In aortic aneurysms, for instance, it is used to develop techniques for rupture risk assessment. In skin, for instance, it is used to assess the effects of freezing and anatomic location, the information useful for donor tissue banks. Planar biaxial testing is one of the most common tools for the mechanical characterization of soft tissues. In this experiment, loadings such as displacements or forces are applied to the edges of the square specimens yielding deformations at the center of the specimens that are measured digitally. Biaxial testing is a great tool as it captures anisotropy and nonlinearity of soft tissues' behaviour and is capable of exploring a wide range of deformation states as it can apply different combinations of loadings. However, because the deformations at the center of the specimens are not controlled, no two mechanical tests are equivalent, complicating the consistency in data extraction and comparison.

In this study, we propose a new approach for biaxial data analysis. First, a surface is fitted to the biaxial data. Second, the mechanical response is interpolated at the true equi-biaxial stretch deformation state (the state at which the deformations at the center of the sample are equal). Third, the effective mechanical properties such as high/low elastic moduli, and transition stretches/stress are extracted from the interpolated response. Other studies, in contrast, extract properties at the equi-biaxial displacement deformation state (the state at which equal strains are applied at the sample edges), which is due to the anisotropy of soft tissues and experimental setup, varies from specimen to specimen. We argue that our proposed approach of data extraction is more robust from the mechanical point of view.

To demonstrate that our proposed approach can result in drastically different data sets, we apply it to previously tested aortic tissues from human donors and pigs. We compare effective mechanical properties extracted from the interpolated equi-biaxial stretch deformation state and conventionally used equi-biaxial displacement deformation state. Statistical analysis shows a significant difference between two groups of mechanical measures whether the measures are compared individually within each group or the general

comparison of groups is conducted. Particularly, measures related to the transition zones (stress/stretch) linked to collagen fibres' engagement behaviour were affected the most. Overall, the results indicate that the way the data is extracted can impact the outcome of biaxial studies. This further highlights the advantage of using the proposed approach of biaxial data extraction at equivalent deformation states versus the conventional approach.

The proposed approach of the data extraction was also applied to human skin samples that came from the same donor's back. Prior to biaxial testing, the samples were frozen/stored using three different freezing protocols (wet freezing in Phosphate Buffered Salin alone and with the cryoprotectant Glycerol as well as dry freezing using Liquid Nitrogen). Then, after testing, the effective mechanical properties were extracted and the effects of freezing and the anatomic locations were evaluated. We found very little quantitive evidence that the freezing storage approach mattered, although some qualitative observations were made to highlight the distinct behaviour of the samples frozen using Liquid Nitrogen. In the case of heterogeneity analysis, samples closer to the spine were different from samples further away from the spine, with the transition zone properties affected the most, especially for the samples subjected to Liquid Nitrogen freezing protocol. Future studies should assess each of the effect of heterogeneity and the effects of freezing separately, however, the overall approach of data extraction seems promising for intra-patient analysis.

**Acknowledgements**

I would like to express my deepest gratitude to all those whose unwavering guidance made this master's thesis possible, and specifically to the mentioned people here.

I am immensely grateful to my dedicated supervisor Professor Taisiya Sigaeva. It was a pleasure to work with such a professional and passionate person whose invaluable guidance, exceptional encouragement and patience throughout the past two years made all of that happen.

Many thanks to the members of my committee, professors, Nima Maftoon and Jason Au for reading my thesis and providing constructive and insightful comments.

A special thank you to my colleague Arya Amiri for his support, help and wide knowledge throughout these two years.

I want to extend my profound gratitude to my parents for their unwavering love, boundless support, and endless encouragement throughout my academic journey from overseas. Their selfless sacrifices, constant belief in my abilities, and words of encouragement have been the driving force behind my accomplishments. Their unwavering faith in me has been a constant source of inspiration, and I am truly grateful for the values they instilled in me and the countless opportunities they provided. I dedicate this thesis to them as a token of my love and appreciation for everything they have done to shape me into the person I am today.

Last but not least, I am thankful for my brother Charbel and his wife Jennifer and my brother Anthony for their help, endless support and encouragement through all the hard times.

## Dedication

To my loving parents, brothers and a special best friend for their sacrifices, support, boundless love and belief in me.

# Table of Contents

# List of Figures

# List of Tables

# List of Abbreviations

**BAV** Bicuspid Aortic Valve 31, 32, 34, 36, 38, 39, 41, 44, 46–48

**HTM** High-strain Tangential Modulus 23–25, 27, 38, 39, 44, 55, 60, 61, 64, 65

**LOESS** Locally Weighted Scatterplot Smoothing 27

**LTM** Low-strain Tangential Modulus 23, 24, 38, 39, 44, 46, 55, 60, 61, 64, 65

**PIG** Porcine Aorta 31, 32, 34, 37–39, 41, 44–48

**TAV** Tricuspid Aortic Valve 31, 32, 34, 35, 38, 39, 41, 44, 47, 48

**TZ** Transition Zone 24, 53, 57, 61, 65

**TZe** Stretch/Stress at the end of the Transition Zone 23, 24, 38, 39, 41, 43, 44, 53, 55, 57–60, 62–64

**TZo** Onset Stretch/Stress of the Transition Zone 23, 24, 34, 38, 39, 41, 43, 53, 55, 57, 58, 60, 62–64

# Chapter 1

# Introduction and Background

The majority of the human body is comprised of soft tissues that serve important mechanical functions [2]. These tissues facilitate various bodily movements, such as the bending of joints, expansion and contraction of blood vessels, and flexibility of the skin. Tissues are composed of various components, including cells, extracellular matrix, oriented fibres, and fluids, which together govern their unique mechanical behaviour. As a result, these soft living materials exhibit different mechanical responses depending on the direction and magnitude of applied loads, necessitating the use of sophisticated testing methodologies to capture their complete mechanical profile.

Mechanical testing plays a crucial role in understanding the mechanical behaviour of soft tissues, which include various biological materials such as tendons, ligaments, muscles, and blood vessels. These tests help researchers and engineers gain insights into the tissue's structural properties, viscoelastic behaviour, and response to external forces. Several methods are employed to conduct mechanical testing on soft tissues going from a microscopic level to a macroscopic level. In this thesis, we aim to explore the mechanical behaviour of various soft tissues through biaxial testing, investigating their anisotropic and nonlinear properties captured through stress-strain relationships. By employing state-of-the-art testing equipment and analysis techniques, we seek to contribute to the existing body of knowledge and advance the field's understanding of soft tissue biaxial mechanics. Furthermore, we aim to bridge the gap between experimental findings and biomedical applications by examining the implications of biaxial testing in the context of aorta and skin tissue biomechanics.

## 1.1 Soft Tissues Mechanical Response

Soft tissues typically exhibit nonlinear, viscoelastic, and anisotropic behaviour, meaning their mechanical response is dependent on the magnitude, duration/rate, and direction of applied forces. This behaviour is governed by the tissue's structural organization and is often observed in the corresponding stress-strain curves, which are a graphical representation of the relationship between the applied stresses (forces per unit area) and the resulting strains (deformations) of material [2]. In addition to cells, which are tissue-specific, the following microstructural components are considered load-bearing in soft tissues: ground substance, elastic fibres and collagen fibres. The behaviour of these components is detailed in the following paragraphs.

Ground substance is constituted of a gel-like substance playing a crucial role in soft tissue's mechanical behaviour. It is known for its isotropic behaviour meaning that it exhibits the same mechanical properties in all directions and also demonstrates nonlinearity in the stress-strain relationship. However, one of the most significant roles of this substance resides in holding the elastic and collagen fibres due to its adhesive function maintaining the structural integrity of the tissues [2, 3]. Several studies investigated the mechanical properties of the ground substance in various soft tissues. For instance, research on articular cartilage demonstrated the nonlinear, time-dependent and strain-rate-dependent behaviour of its ground substance affecting its viscoelastic properties [4].

Elastin is a highly elastic protein found in soft biological tissues, specifically in skin and aorta. Elastic fibres are composed of elastin and are responsible for the elasticity and recoil properties of these tissues [5]. These elastic fibres typically dominate the overall mechanical

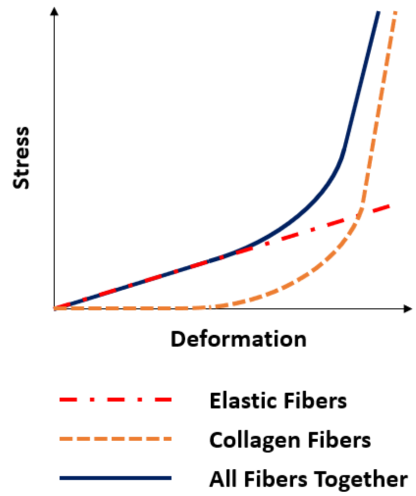


Figure 1.1: Elastic and Collagen fibres' generalized response to loading resulting in soft tissues' nonlinear curves.

response at low levels of deformation. And when loaded, they respond to loads linearly establishing a linear slope at the beginning of the stress-deformation curve, known as the elastic or linear region (see figure 1.1). In this region, the fibres exhibit elastic behaviour, meaning they can deform reversibly without permanent changes. The linear slope in this region indicates the stiffness or modulus of elasticity of the elastic fibres, reflecting the tissues' resistance to deformation under low-stress conditions [5, 6]. It is a challenge to distinguish the response of the ground substance and elastic fibres at a low strain regime, so these load-bearing microstructural components are often combined in modelling.

Unlike elastic fibres, collagen fibres are responsible for both the transition zone and the linear region located after it (see figure 1.1). These fibres exhibit a wavy configuration in the undeformed state which results from their hierarchical structure and allows them to accommodate deformations [7]. Collagen fibres also show a specific orientation within soft tissues. They also do not respond to loads until nearly or fully straightened which does not usually happen at the low deformation regime (beginning of the stress-deformation curve). At the transition zone, when large/moderate loading is applied, these collagen fibres start to gradually recruit by losing their waviness throughout this zone: the more fibre straighten up, the stiffer the transition zone becomes [8, 9]. Once all fibres are fully straightened, the transition zone ends and the linear region at the end of the stress-deformation curve is formed [10–12].

In combination, collagen and elastic fibres define the fibre-related nonlinearity of the stress-deformation curve as illustrated in figure 1.1 showing the generalized response of these fibres in soft biological tissues. However, the overall response is tissue-specific due to the different elastin and collagen ratios between soft tissues [13]. Further, this fibrous behaviour is superimposed on the nonlinear response of the isotropic ground substance fully defining the final stress-deformation curves (not shown here). Additionally, elastic and collagen fibres often exhibit anisotropic behaviour, meaning that their mechanical properties vary depending on the direction in which they are loaded or stretched. This anisotropy arises due to the structural arrangement of the fibres and their orientation within the tissue. Fibres may be aligned or organized in a specific pattern, resulting in different mechanical responses along different directions. When characterizing the stress-deformation curves in different directions, the same process is repeated. All characteristics of the curves (tangents of the linear slopes of transition zone characteristics) are evaluated separately for each direction. This allows for the assessment of anisotropic behaviour and the determination of mechanical properties specific to each direction [11, 14].

## 1.2 Methods for Mechanical Testing

There are different mechanical tests to capture soft tissue biomechanical response such as stress/force measure vs deformation. In this section, different testing techniques used in the literature are presented starting from the basic methods and ending with biaxial testing which has gained the most interest in the course of this thesis.

First, one of the testing methods used in that field is shear wave elastography. It represents an imaging-based technique used to evaluate the mechanical properties of soft tissues. It uses ultrasound or MRI to induce shear waves in the tissue and measures their propagation speed, which is related to the tissue's stiffness or elasticity. Shear wave elastography has gained popularity for assessing the mechanical properties of muscles, tendons, and other soft tissues [15, 16]. However, this testing technique is not widely spread due to technical constraints, such as the MRI's bad resolution as well as its high cost [17]. Another limitation encountered in some studies [18] is the failure to maintain the skin tension leading to a decrease in the skin's shear wave elastography's reproducibility.

Next, one other popular method is bulge testing. Bulge testing is a common method used to characterize the mechanical properties of thin, compliant membranes or tissues, such as aortic valves or bladder tissues. In this test, the specimen is clamped along its edges and pressurized, causing it to bulge outward. One can determine parameters such as the elastic modulus, burst pressure, and thickness-dependent behaviour of the material by measuring the bulge profile and relating it to the applied pressure [2]. However, this technique presents some challenges such as the dependency of Young's modulus on the accuracy of the thickness measurement, in addition to the inaccuracy in the deflection amplitude determination [19].

Next, compression testing involves applying a compressive load to a tissue sample to determine its compressive properties, including compressive strength, elastic modulus, and stress-strain behaviour. This test is commonly used for cartilage and soft tissue applications [20, 21]. However, for planar soft tissues it is associated with several limitations such as the effect of sample size and inability to properly secure a sample for experiment [22].

In addition to all of that, shear testing evaluates the tissue's response to shear forces by applying forces parallel to the tissue plane. It provides insights into the tissue's shear modulus, strength, and viscoelastic properties. Shear testing is essential for understanding the behaviour of materials like skin and subcutaneous tissue [2, 21]. Similarly to the previous mechanical test, shear is hard to implement in planar soft tissues as it is hard to secure the sample and make measurements [23].

Another test mentioned in the literature is indentation testing. This technique involves applying a controlled force to the tissue surface and measuring the resulting deformation. It provides information about the tissue's mechanical properties, such as stiffness, viscoelastic behaviour, and depth-dependent characteristics. Indentation testing is also widely used to assess the mechanical properties of soft tissues such as articular cartilage [24]. However, the results highly depend on the indenter size, shape and depth of indentation [25].

Tensile testing is arguably the most popular mechanical testing method used for the mechanical characterization of soft tissues, especially for planar ones. In tensile tests, tissue is subjected to stretching forces. Uniaxial tensile testing is a method that involves applying an axial load to a tissue strip (usually until failure) while measuring the resulting deformation. It provides information about the tissue's tensile strength, elastic modulus, ultimate stress, and strain behaviour along the loading axis [2, 26]. To obtain anisotropic behaviour differently oriented strips should be tested. On the other hand, in biaxial testing, a tissue sample is subjected to loading along two orthogonal axes. This method more accurately represents the complex stress and strain states experienced by most soft tissues in vivo. Biaxial testing enables the evaluation of anisotropic properties and is particularly useful for characterizing the mechanical behaviour of tissues such as blood vessels and cardiac tissues [2, 27]. This testing method constitutes a significant part of this thesis and will be more detailed in the next section.

## 1.3 Biaxial Testing and Data Inconsistency Issue

Biaxial testing is a method used to analyze the mechanical behaviour of soft biological tissues under in-plane stress due to forces applied in two perpendicular directions. The history of biaxial testing can be traced back to the early 20th century when researchers began to recognize the importance of understanding material responses to complex stress states. *Field et al.* mentioned that the first report of biaxial testing was in 1957 [28]. Over the years, various types of biaxial testing equipment and techniques have been developed. These advancements have provided valuable insights into the mechanical properties of materials and have been instrumental in the development of engineering design codes and standards. Today, biaxial testing continues to be an active area of research, with applications ranging from material characterization to the design of structural components [29].

Biaxial testing is often applied to soft biological tissues which typically involves using a specialized mechanical testing rig [27]. It allows for the characterization of various mechanical properties of soft biological tissues, including their elastic modulus, stiffness, and ultimate strength in different directions. By applying loads along two orthogonal axes, researchers can assess the anisotropic behaviour of tissues, which is crucial for understanding their physiological function and designing tissue-engineered constructs. *Lanir* & *Fung* have demonstrated this in most of their studies. For instance, they conducted research on rabbit skin where biaxial testing was employed to retrieve its mechanical properties [30]. In [31, 32] biaxial testing was used to understand tissue structure-function relationships. *Sacks et al.* used biaxial testing to facilitate the design of tissue scaffolds with desired mechanical properties [33].

Biaxial testing provides good coverage of stress-deformation data points that help in modelling the mechanical behaviour of soft biological tissues. This data contribute to the development of constitutive models for tissue simulation and computational modelling [27,34,35]. Constitutive models are essentially complex mathematical expressions allowing to relate stresses and deformation via material constants. Even if the expressions are pre-defined, it is often a challenge to select a suitable constitutive model and implement an optimization algorithm to fit experimental data and find material constants. Many biomedical engineering studies that conduct biaxial testing for many specimens usually limit themselves to reporting effective mechanical properties such as tangent moduli that come from biaxial tests rather than resort to constitutive modelling. One of the reasons is perhaps the fact that material constants are often either dependent or do not have clear physical meaning and thus are not suitable to draw any scientific conclusions unless finite element simulations are performed.

Importantly, there is currently no standardized method of either biaxial testing or biaxial data analysis in the field. The tissue sample, often in the form of a square or cruciform shape, is secured to a biaxial testing device with clamps or sutures. Controlled loadings (either displacements or forces) are then applied independently along two orthogonal axes, typically using computer-controlled motors or pneumatic actuators. The resulting deformation is measured using a variety of techniques, such as video-based systems or digital image correlation (DIC). Because deformations are not controlled and the response of the specimens depends on the orientation/configuration of fibres, there are no two specimens with the same deformations captured by DIC. This raises the issue - how can researchers extract such properties as tangent moduli from two specimens and compare them if the specimens' deformation states are not comparable? The overwhelming majority of the studies simply ignore this inconsistency [36–42]. Only a few researchers briefly discuss it and actually tackle it. Some resorted to first conducting constitutive modelling and then extracting properties at the equivalent deformation states from the model [1, 43–45]. However, this approach is often cumbersome and depends on the quality of the constitutive model fitting. For instance, if the fit is just acceptable and not perfect, the accuracy of the extracted properties will be affected. A few other researchers have suggested bypassing constitutive modelling and simply interpolating the response at the equivalent deformation states using 3D surfaces fitted to 3D biaxial data [46, 47]. This approach seems the best way to ensure consistency in data extraction but it did not gain popularity yet. Perhaps one of the reasons is the fact that no one specifically reported how the outcome of any biaxial study can change when matched vs. unmatched deformation states are used for data extraction.

## 1.4 Biomechanics of Aortic Tissue and the Importance of Biaxial Testing in its Properties' Characterization

The aorta is the largest artery in a living organism. It is a major blood vessel that carries oxygenated blood from the heart to the rest of the body [48] through smaller branching arteries [49]. Aortic tissue biomechanics play a crucial role in understanding the mechanical behaviour of the aorta. Unlike other arteries, the aorta is divided into several major segments: the ascending aorta, the aortic arch, the descending aorta and the abdominal aorta [50]. Interestingly, the aorta possesses unique biomechanical properties that allow it to withstand the strong pulsatile flow of blood directly from the heart and maintain its structural integrity [51]. Similarly to most soft biological tissues, the aorta comprises elastic fibres, collagen fibres, and smooth muscle cells that enable this biomechanical behaviour. The elastic fibres provide the aorta with elasticity, enabling stretching during systole (ventricular contraction) and recoiling during diastole (ventricular relaxation). The collagen fibres provide tensile strength to the vessel, thereby both types of fibres contribute to maintaining continuous blood flow [52]. An additional unique feature of the aorta is that it contacts aortic valves that prevent the reverse flow of blood back into the heart [53]. One aspect of the aorta is the pathology called aneurysm. An aneurysm refers to the localized dilation or bulging of an arterial wall, commonly occurring in older patients [54]. It is a significant health concern as it can lead to life-threatening complications such as rupture, which carries a high mortality rate. Early detection and monitoring of aneurysms are crucial for timely intervention and prevention of complications [55–58].

Biaxial testing is a commonly used experimental technique to investigate the mechanical properties of aorta tissue. This testing method is used due to its ability in simulating more realistic multi-axial loading conditions of the aorta mimicking its in-vivo behaviour [41,59]. In this approach, valuable insights are provided into the anisotropic and nonlinear nature of aortic tissue, as well as its response to different physiological and pathological conditions. The mechanical behaviour of the aorta is influenced by various factors, including the composition and arrangement of its extracellular matrix, elastin fibres, collagen fibres, smooth muscle cells, and endothelial cells. In the literature, several studies have investigated aorta tissue biomechanics through biaxial testing. These studies provide valuable insights into the mechanical behaviour of the aorta and reveal how important this test is in the extraction of its mechanical properties. For example, a study by *Holzapfel et al.* investigated the anisotropic mechanical properties of human thoracic aorta tissue using biaxial testing. The results revealed that the aorta exhibits pronounced anisotropy, with the stiffness and strength varying significantly with the direction of loading [60]. Another study by *Kamenskiy et al.* [61] biaxially tested different types of arteries such as the thoracic and abdominal aorta, common carotid, etc. Most of the results showed a nonlinear and anisotropic behaviour with the common carotid being the least anisotropic. Interestingly, the effect of freezing also made its way into some studies where *Matsumoto et al.* conducted biaxial testing on fresh and frozen porcine thoracic aneurysms. The samples were tested at both room temperature and 37° C. The results showed that the elastic modulus and the anisotropy were not influenced by the followed protocol [43]. Another biaxial study was also conducted on human abdominal aortic aneurysm intraluminal thrombus (ILT) by *Siobhan et al.* [62] where the effect of freezing on the mechanical properties of the ILT.

## 1.5 Biomechanics of Skin Tissue and the Importance of Biaxial Testing in its Properties' Characterization

The human skin is a complex and remarkable organ that serves as the body's first line of defence against external threats. Composed of several layers, each with unique characteristics and functions, the skin plays a vital role in protecting underlying tissues, regulating body temperature, and facilitating sensory perception [63–65]. Interestingly, skin exhibits a specific mechanical behaviour revealing its non-linearity, viscoelasticity and anisotropy. First, the non-linearity of skin, especially observed in the stress-deformation curves, is due to the elastic but mostly collagen fibres integrated into its microstructure [35]. The skin is known to be highly viscoelastic [66, 67], which is often demonstrated through creep tests [68, 69]. A study by *Karimi et al.* showed the relaxation behaviour of rat back and abdomen skin after being extended and held at a constant displacement [70]. Finally, anisotropy, physically known as the difference in the behaviour of skin in different directions [71], is widely reported through what is known as Langer lines [72] which define the orientation of collagen fibres or natural tension lines [71, 73, 74]. Skin biomechanical characterization is vital in many applications. Starting with needle insertion, many studies simulated this process requiring precise mechanical properties of human skin [75–77]. As another example, skin biomechanics is important for tissue engineering as autografts can be optimized to reduce the risk of complications in transplantation [78].

Biaxial testing is a significant part of skin biomechanics. In the literature, it was proved that the in-vivo behaviour of skin can be characterized by biaxial testing revealing its importance in that field [30, 79]. It allows researchers to assess its mechanical properties, such as tensile strength, elasticity, and deformation behaviour of skin (see section 1.3). Strikingly, *Lanir* and *Fung* was the first to develop a biaxial testing setup aimed to be conducted on skin to describe its 3D behaviour [80]. It was used by several studies by applying it on rabbit skin to evaluate its tensile and relaxation behaviour [30], as well as the human skin mechanical characterization [81]. In contrast, a study by *Holzapfel et al.* mentioned that biaxial testing is not a sufficient technique to fully characterize the skin properties [82, 83]. On the other side, studies also evaluated the effect of freezing on skin samples. For example, a biaxial study was conducted on bat wing skin where frozen samples were tested and the results revealed the characterized deformation, mechanical properties and fibres distribution [84]. However, nowadays, biaxial testing is one of the most used techniques in that manner as a significant number of studies rely on it considering the fact that it mimics the in-vivo behaviour of skin very well.

## 1.6 Effect of Mechanical Heterogeneity in Skin and Aorta

After investigating the skin and aorta structures and evaluating the importance of biaxial testing in their mechanical characterization, the heterogeneity of both these tissues will be detailed in this section. Heterogeneity refers to the presence of variations or differences within a particular entity or system. In the context of biological tissues and organs such as the aorta and skin, heterogeneity can arise at different levels, including cellular, molecular, and biomechanical characteristics. Aorta, for instance, exhibits inherent heterogeneity across its various segments and layers [85]. For example, the ascending aorta has a higher proportion of elastic fibres in the tunica media compared to the abdominal aorta, which has a higher content of collagen fibres [86]. This regional heterogeneity influences the mechanical properties and response to hemodynamic forces along the length of the aorta.

Similar to the aorta, the skin also exhibits heterogeneity in its structure and function. Different regions of the skin, such as the face, palms, and soles, have distinct characteristics in terms of thickness, hair follicle density, and sweat gland distribution. The skin's dermis layer shows variations in collagen and elastin content, influencing its mechanical properties and elasticity [87–89].

Understanding and characterizing the heterogeneity of the aorta and skin is essential for unravelling the complexities of tissue function, development, and disease progression.

## 1.7 Effect of Freezing on Biomechanics of Skin and Aorta

In addition to the effects of heterogeneity, an important factor that can be studied through biaxial testing is the effects of freezing on soft tissues. The process of freezing is widely employed as a preservation technique for soft tissues. On the one hand, freezing is often needed to transport tissue for further usage in research [90,91], as it helps to retain tissues' structure and integrity. Aortic tissues, for instance, are often frozen before further research is done [92]. On the other hand, freezing is the standard procedure for tissue banks, where, for instance, donors' skins are stored before being turned into skin grafts for burns treatment [93, 94].

Freezing involves decreasing the temperature of a substance below its freezing point, which, in the case of soft tissues, can irreversibly change its biomechanical properties. One of the intermediate effects is that freezing can cause changes in tissue stiffness [95] - the decrease in elastic moduli has been reported [96]. Next, certain freezing protocols such as rapid freezing can result in ice crystal formation, which may cause structural damage to the tissue. This damage can affect the integrity and mechanical behaviour of the sample during biaxial testing [97]. On the other hand, long-term effects rely on prolonged freezing which can lead to tissue degradation over time, affecting the overall mechanical properties. *Woo et al.* concluded that tissues frozen for a longer time might lead to loss of hydration which can affect the tissue's mechanical behaviour, such as its compliance and viscoelastic properties [98].

Various freezing techniques are being used to preserve tissues' mechanical properties - from the utilization of cryoprotectants to the usage of liquid nitrogen. The study focusing on the investigation of different effects of freezing protocols can shed light on the best freezing-storage practices that will minimize changes in tissue biomechanics.

# Chapter 2

# Rationale and Objectives

## 2.1 Rationale

The rationale for the present thesis stems from the existing challenges and inconsistencies in the interpretation of biaxial testing data within the scientific field of soft tissue biomechanics. Biaxial testing offers numerous benefits in understanding the mechanical properties of soft biological tissues. However, the lack of consistency in data interpretation poses a significant obstacle. Constitutive modelling is a commonly employed approach where experimental data is fitted to a surface, which is then utilized for finite element analysis. While this method can provide valuable insights, it often requires assumptions and may not accurately capture the true mechanical behaviour of the tissue. On the other hand, researchers in the biomedical field often focus on extracting specific mechanical properties directly from the biaxial data, such as stiffness or anisotropic parameters. However, the inherent variability in deformation fields across different tests makes it challenging to ensure consistent testing conditions between samples.

## 2.2 Objectives

The objective of the present thesis is to address these limitations and enhance the technique for extracting data from biaxial testing. By ensuring data is extracted at an equivalent deformation state, researchers can bypass the need for constitutive modelling and obtain more accurate and reliable insights into the mechanical properties of soft biological tissues. This research aims to contribute to the field by providing a more standardized and consistent approach to biaxial testing, ultimately advancing our understanding of soft tissue mechanics and potentially informing biomedical applications.

**Objective 1: Develop a robust and consistent approach to properly extract mechanical properties from biaxial testing data.**
Because the deformations at the center of the specimen can not be controlled in biaxial testing, it is vital to extract properties at the equivalent deformation states for proper data collection. Hence we propose and implement a new surface fitting approach using MATLAB (version R2022b). A new GUI is developed to effortlessly plot the tested tissue's 3D data and fit a surface to it. This enables the possibility to extract the required mechanical properties and run an analysis.

**Objective 2: Analyze data provided from the previous studies and prove that the proposed method of data extraction can lead to significant changes in the results and thus is recommended to improve the accuracy of any biaxial study.**
After the fulfilment of the first objective, data for different previously tested aortic samples are used and statistically analyzed to assess this new technique. The resulting effective mechanical properties are extracted using the aforementioned approach and the conventional approach. The objective is to analyze these properties and aims to prove the hypothesis by finding the significant differences between these two approaches for the datasets available at the time of launching this research project.

**Objective 3: Apply the newly implemented approach and assess its effectiveness in the evaluation of small differences within the same tissue by investigating the effects of heterogeneity and freezing protocol.**
A human donor's skin specimens were frozen then tested and analyzed. The surface fitting approach was employed and, similarly, effective mechanical properties were extracted using both the conventional and advanced data extraction approaches. This study enabled the possibility to evaluate if this advanced extraction data approach is more robust and holds great potential for studies centred on detecting subtle differences among diverse groups of specimens within the same patient. In particular, this includes examining the impacts of heterogeneity and the choice of the freezing/storage protocol.

# Chapter 3

# Methodology

## 3.1 Objective

In this section, the first objective proposed in the previous Chapter 2 will be fulfilled. We first discuss the basics of biaxial testing and biaxial data analysis. We show how stress-deformation curves are derived. Then, we discuss how the conventional method of extracting effective mechanical properties is conducted and highlight possible issues with such an extraction method. Finally, we propose the more appropriate methodology for data extraction, share the details of the developed GUI that applies this method and outline statistical means that will be used in the following chapters to assess the effectiveness of this method.

## 3.2 Biaixial tensile testing

In this thesis, the results from two different biaxial testing setups were utilized: ElectroForce Systems (TA Instruments, Springfield, MO, USA) shown in figure 3.1a was used in Chapter 4, and Cellscale Biotester 5000 (Cellscale Biomaterial Testing, Waterloo, Canada) shown in figure 3.1b was utilized in Chapter 5. Although these setups differ in their specific design and capabilities, the underlying principles of operation, experimental procedure, and mechanical data analysis approaches are similar. Therefore, the common methodology will be described in this section for a generic tissue, and any specific tissue-, equipment- or/and experimental protocol-related differences will be outlined in respective Chapters 4 and 5.

### 3.2.1 Specimen preparation

The biaxial machine employed in the experiments consists of four linear actuators and two load cells to simultaneously extend a tissue sample in two orthogonal directions (labelled "11" and "22") and record corresponding forces ($F_{11}$ and $F_{22}$ in figures 3.1c and 3.1d). The sample is square-shaped and typically measures 10 to 20 mm on each side, depending on the tissue and study purpose. The thickness of the specimen, $H$, ranging from 0.1 to 4mm for planar tissues suitable for biaxial testing, is measured before the experiment by either a calliper or thickness gauge. Typically, the specimen is marked to identify the orientation - in our case, the dot is placed in the top right corner to specify that the horizontal direction corresponds to "11" and the vertical direction corresponds to "22".

As a part of specimen pre-processing, four hooks (two pairs of suture-connected hooks) are commonly placed 1-2 mm away from the edge at equal distances along each specimen side. For smaller specimens, two suture-connected hooks per side can be deemed sufficient (see figure 3.1e ). Then, the specimen reference dimensions, denoted as $L_{11}$ and $L_{22}$, are measured along two orthogonal directions as distances between the sets of the opposite hooks. Also, the central part of the specimen is marked by either dots or speckles to enable deformation tracking. These are all shown in figures 3.1e and 3.1f.

Next, sutures connecting pairs of hooks are used to mount the specimen to the linear actuators through a pair of pulleys (figures 3.1c and 3.1d). The mounted specimen is then submerged in a temperature-controlled bath at $37°C$, simulating in vivo conditions and maintaining a physiological environment. Finally, a camera is positioned above the

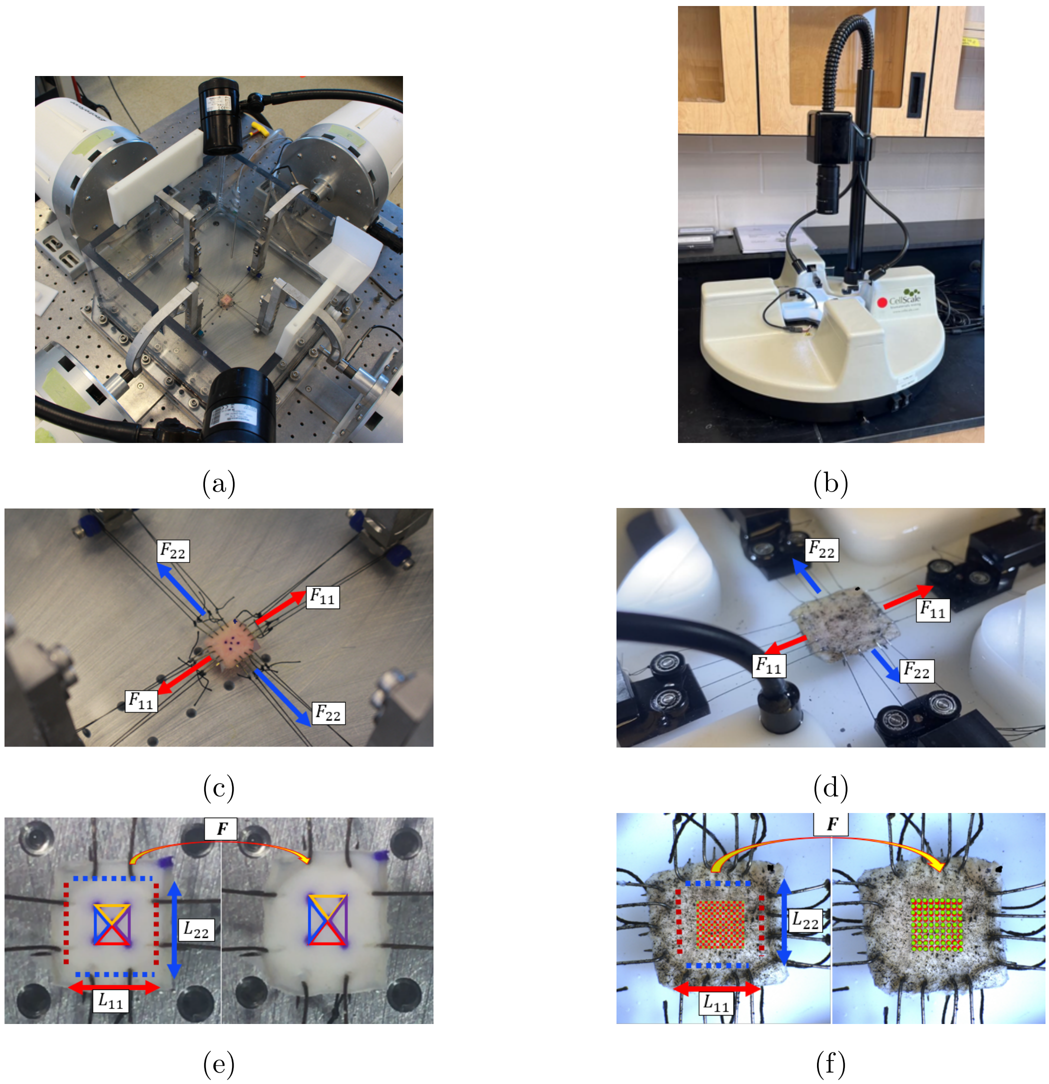


Figure 3.1: Different biaxial machine setups: (a) ElectroForce Systems biaxial machine, (b) Cellscale's Biotester 5000, (c) Forces applied using ElectroForce Systems in the horizontal (11) direction and vertical (22) direction (image from [1] is edited and used with permission issued by Elsevier), (d) Forces applied using Biotester 5000 in the horizontal (11) direction and vertical (22) direction, (e) Displacement and deformations tensor using ElectroForce Systems, and (f) Displacement and deformations tensor using Biotester 5000

specimen to record it at all times, and the experiment is ready to be launched (figures 3.1a and 3.1b).

### 3.2.2 Testing protocol

The experimental protocol is set as follows. First, the sample is preloaded to eliminate any tissue slack. Next, the desired displacements in the orthogonal directions are assigned. Because different specimens have different referential dimensions, for consistency, the strains are used. First, the equi-biaxial displacement protocol, labelled as "1:1", ensures the strain applied in direction "11" is equal to the one in direction "22". The displacement $\delta$ corresponding to the desired maximum strain $\varepsilon_{L_{ii}}$ is calculated based on the referential distances $L_{11}$ and $L_{22}$ as $\delta = \varepsilon_{L_{ii}} \cdot L_{ii},\ ii = \{11, 22\}$. For instance, if $L_{11}$ and $L_{22}$ are both 10 mm, and the maximum desired strain is 60%, each arm of the sample is simultaneously extended by 3 mm, resulting in a total displacement of $\delta = 6$ mm in each direction. The loading and unloading process is repeated several times to ensure the repeatability of the sample's response. The length of the loading/unloading cycle can be set to ensure a specific loading rate. Next, the process is repeated for other non-equibiaxial displacement protocols to explore tissue response at different deformations states. Typically, protocols "1:0.5", "1:075", "0.5:1", and "0.75:1" are adopted, where the first number is the fraction of the maximum strain in "11" direction, and the second number is the fraction of the maximum strain in "22" direction. For instance, for the example earlier, protocol "1:0.5" corresponds to 60% strain in "11" direction and 30% strain in "22" direction. The explored deformation range can be seen in figure 3.2a.

## 3.3 Biaixial data analysis

### 3.3.1 Derivation of stress-deformation curves

The machine records displacements ($\delta_{ii},\ ii = \{11, 22\}$) and forces ($F_{ii},\ ii = \{11, 22\}$) for each experimental protocol. The actual data to produce stress-deformation curves is collected only from one of the last loading cycles where the tissue is sufficiently preconditioned.

The First Piola-Kirchhoff Stresses in "11" and "22" directions are calculated as the forces divided by the undeformed tissue cross-section areas to which they are applied (measured beforehand as the referential geometry):

$$P_{11} = \frac{F_{11}}{L_{22} \cdot H}, \quad P_{22} = \frac{F_{22}}{L_{11} \cdot H}. \tag{3.1}$$

Although the assigned displacements $\delta_{ii},\ ii = \{11, 22\}$ are intended to achieve the desired maximum strain based on the referential dimensions $\varepsilon_{L_{ii}},\ ii = \{11, 22\}$, it is widely acknowledged in the field that the strains at the edges of a sample are affected by boundary conditions [99–101]. Therefore, measuring deformations at the specimen's center, where they are presumably more homogeneous and unaffected by the boundary effects, using means of Digital Image Correlation (DIC), is a common practice. Two commonly used approaches for tracking such deformations are the utilization of graphite speckles and marker dots, which are placed at the center of the specimen (see figure 3.1c and 3.1d) and photographed at the specified frequency throughout the experiment. DIC is then used to optically track how the location of either marker dots (see figure 3.1c) or speckles (see figure 3.1d) change with loading. Depending on the approach, either $j$ triangle or $j$ square elements are used to mesh the tracked surface, and changes in the distances between sides of these shapes are used to calculate the local in-plane deformation gradients $\boldsymbol{F}_j$[†] [‡]. These local deformation gradients are then averaged across all elements of the mesh to produce the averaged deformation gradient

$$\boldsymbol{F} = \begin{bmatrix} \lambda_{11} & F_{12} \approx 0 \\ F_{21} \approx 0 & \lambda_{22} \end{bmatrix}.$$

Here the non-diagonal element $F_{12}$ and $F_{21}$ are the shear deformations, that are relatively small in the biaxial testing and are, therefore, neglected. Because of this assumption, the diagonal elements representing the stretches in the horizontal and vertical directions, respectively, can be assumed to be "principal" stretches. These exact stretches, collected from the selected loading cycle, are plotted against the first Piola-Kirchhoff stresses (equations 3.1) to produce stress-deformation curves.

Notably, in contrast to the strains assigned at the border of the specimen $\varepsilon_{L_{ii}}$, $ii = \{11, 22\}$, the stretches $\lambda_{11}$ and $\lambda_{22}$ calculated at the center of the specimen reflect the tissue's localized properties such as nonlinearity and orientation of fibres that are unique for specific tissue, specimen and tracked specimen's surface region. One can refer to figure 3.2a to see how the assigned deformations at the edges shown in figure 3.2b produce a unique deformation field at the center of the specimen. Hence one can conclude that the deformation ranges explored in two different tissue specimens tested biaxially are always different even if the experimental protocol is the same.

## 3.4 Effective mechanical properties

After completing biaxial testing and deriving stress-strain curves, it is a common practice to extract mechanical properties from these curves for various grouped specimens and

[†]The actual deformation gradient in the biaxial testing is three-dimensional with the out-of-plane component calculated from the incompressibility condition.

[‡]There is no agreement on whether dot markers or speckles produce better results as there are advantages and disadvantages of each method for specific tissue/application [102, 103].

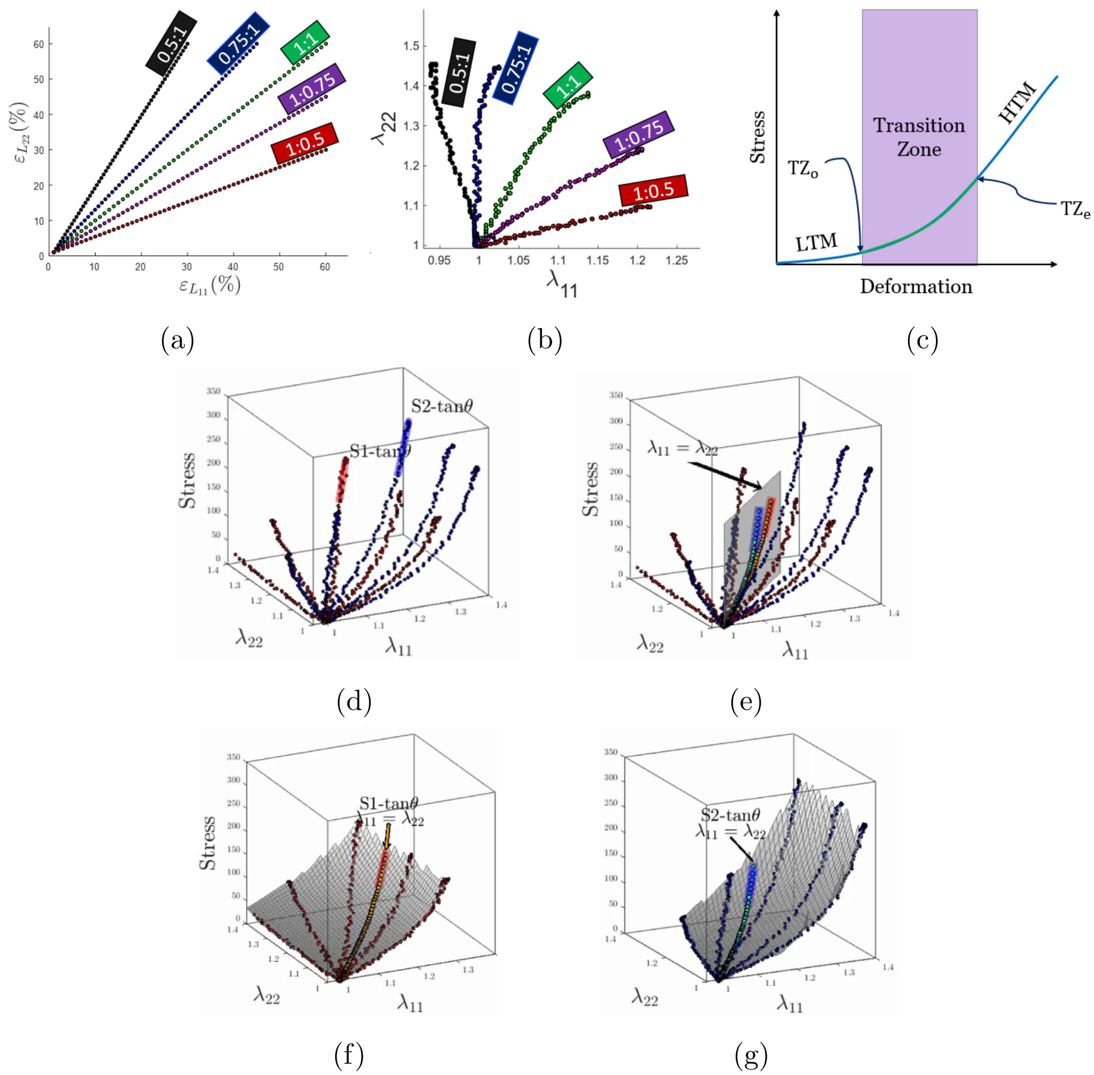


Figure 3.2: (a) Assigned deformations related to each protocol. (b) Unique actual deformations of a sample. (c) Sketch defining the different mechanical properties: TZo, TZe, LTM and HTM. (d) The difference shown by overlapping two samples by emphasizing on the tangent moduli in blue and red. (e) The equistretches/interpolated curves after overlapping the same two samples and showing that these curves are in the same plane. (f) Surface fitted to a set of five protocols' data showing the envelope shape in the "11" direction. (g) Surface fitted to a set of five protocols' data showing the envelope shape in the "22' direction.

statistically compare them. Conventionally, stress-deformation curves corresponding to the equi-biaxial displacement protocol $\varepsilon_{L_{11}} = \varepsilon_{L_{22}}$ (protocol "1:1") are used for extraction. For instance, a green line in figure 3.2a corresponds to the strains assigned at the border for protocol "1:1", while in figure 3.2b, it corresponds to the deformation (stretches) produced at the center of the specimen, and finally, in figure 3.2c, it corresponds to one of two directional stress-deformation curve produced. From the latter curve, effective mechanical properties associated with the corresponding direction are conventionally extracted.

There are a few effective mechanical properties of interest that can be extracted from the stress-deformation curves, and they are associated with the behaviour of load-bearing microstructure, which has been discussed in Chapter 1.1 and figure 1.1. Starting from the beginning of the stress-deformation curves (figure 3.2c) - LTM or, simply, initial slope, can be extracted. This effective property is usually associated with the combined behaviour of elastic fibres and ground substance. Next, the initial linear slope is followed by Transition Zone (TZ), dominated by gradually engaging collagen fibres. Such effective mechanical properties as TZo and TZe are useful in characterizing collagen fibre recruitment behaviour. Finally, when all collagen fibres are engaged, the transition zone is replaced by the linear zone with the HTM. This effective mechanical property characterizes the stiffness of engaged collagen fibres [104].

When the effective mechanical properties are extracted from one direction, i.e., $P_{11} - \lambda_{11}$ stress deformation curve, the process is repeated for the other direction as well ($P_{22} - \lambda_{22}$). One of the simplest ways to analyze anisotropy is to look at the ratios of effective mechanical properties in two directions, i.e., dividing a specific property in the direction "11" by the same property in the direction "22". In general, if the ratio outcome is close to 1, the property is said to be isotropic, otherwise - anisotropic. However, even this measure is relative and it depends on the variability within the specific effective mechanical property. For example, in the case of stretches where the values and variability are considerably small (1-1.1), the determined ratios can always be fairly close to 1. In this case, the values very close to 1 indicate isotropy (e.g., 0.99). The further the ratios will get from 1 will indicate an anisotropic behaviour (for example, a ratio of 0.95 would be anisotropic in that case).

HTM values vary much more, for example, from 2000 KPa to 8000 KPa, and, therefore, the ratios wouldn't be as close to 1 compared to stretches. Therefore, for this effective property, a ratio of 0.95 would indicate a fairly isotropic behaviour, while a ratio larger than 2 or less than 0.5 would indicate that one direction is twice as stiff as the other one. Notably, there is no agreement in the literature on how to define anisotropy so we used the simplest definition [33, 105].

Importantly, due to nonlinearity and anisotropy, each soft biological tissue sample produces a unique deformation state where the effective properties discussed earlier are compared. For example, in figure 3.2d, two different samples' stress-strain curves were overlapped. This highlights the difference observed through HTM and emphasizes the fact that no two samples will lead to the same deformations at the center which is the central issue raised in this thesis. There is a need to extract these properties at the equivalent deformation states $\lambda_{11} = \lambda_{22}$ which are not captured through biaxial testing (see figure 3.2e). There are two approaches to do that - through constitutive modelling as described in the introduction which is out of the scope of this thesis and through interpolation from surface fitting which is detailed in the following section (3.5).

## 3.5 Surface Fitting

Given that sufficient data is available from biaxial testing, three-dimensional curves can be plotted representing the response of soft biological tissue to each applied protocol. These curves show the envelope shape to which a surface can be fitted (see figure 3.2f and 3.2g). Therefore, from this surface, the interpolated protocol can be extracted, and repeating this process on different specimens results in consistent deformation states from which the effective mechanical properties can be extracted. From now on, and for the rest of this thesis, the conventional approach of extracting data from protocol "1:1" will be referred to as the "experimental protocol" or "Exp" because it represents the actual curves resulting from the data collected after an experiment. And the proposed method of extracting data from the curve interpolated from the surface fitted to the data will be referred to as the "interpolated protocol" or "Interp".

The proposed surface fitting method was implemented into MATLAB (version R2022b), for which a GUI was developed. The outline of this GUI is shown in figure 3.3 and comprises different features. First, running the program enables the possibility to select the desired set of data to analyze. After the data is plotted, and in case any protocol appears to be either irrelevant or ill-behaved, the user will have the choice to drop it. To facilitate this process, stretches are also plotted in 2D (see Graph 3 figure 3.3. Then, the surface can be fitted to the data (Graph 1 and 2 figure 3.3). Three different MATLAB built-in surface types are available: Linear, Cubic and Lowess. These fit types include an option to modify the number of points resulting in a mesh increase for higher accuracy. As soon as the surface is fitted, the interpolated protocol corresponding to $\lambda_{11} = \lambda_{22}$ is displayed in both 2D (Graph 4 figure 3.3) and 3D (Graph 1 and 2 figure 3.3). Toggling the "closest protocol" button will plot the closest protocol to the interpolated response in 2D (Graph 4 figure 3.3). This feature helps ensure that the characteristics of the curves were preserved by the surface. Next, effective mechanical properties can now be generated by ticking the desired property in the "Effective Mechanical Properties" tab. An option to get smoother curves is also included in this GUI. Also, this interface comprises different buttons located at the bottom: the "Open" button makes it easier to jump to a new set of data by selecting a new sample's folder, and the "Refresh" button makes it either to apply and show any modified inputs the user selects on the interface. The "Save" button saves the last 2D plot showing the interpolated response, as well as all its data points. Finally, to quit the GUI, the "Quit" button can be used.

To elaborate more on the surface fitting approach, linear fitting is a widely used method to fit a straight line to a set of data points using linear regression [106] where an assumption of a linear relationship is made between the dependent and independent variables. For instance, stretches constitute the dependent variables, while stresses represent the independent variables. An extension of linear regression is called linear surface regression using a linear function to determine a plane that best fits 3D data points. Next, cubic fitting is based on the same concept of plane fitting in a three-dimensional space using cubic polynomials. It is more relevant and useful when it comes to complex patterns and curvatures in the available data [107]. Last but not least, Locally Weighted Scatterplot Smoothing (LOESS) consists of fitting a weighted polynomial regression to datasets by giving higher weight to closer points and lower weight to distant points. Similarly to cubic, it is also useful when having complex and nonlinear data [108, 109]. Any of the proposed surface fitting approaches can be used but some work better for more curves with more pronounced nonlinearity, others - for curves with less pronounced nonlinearity.

This GUI and data extraction approach are tested in Chapters 4 and 5. By employing the interpolated response specific to each data set and employing the experimental protocol "1:1", the relevant effective mechanical properties such as low/high elastic moduli and transition stretches/stresses can be successfully extracted. One can also introduce an interesting parameter - "percentage difference" which is defined in this thesis as the ratio of a property's interpolated response subtracted from its experimental response, then divided again by its experimental response. This ratio results in a numeric value reported in (%) showing how significant the observed difference is. For example, the percentage difference for HTM1 is defined as follows:

$$\mathrm{HTM1}_{\text{percent diff}} = \frac{\mathrm{HTM1}_{\mathrm{Exp}} - \mathrm{HTM1}_{\mathrm{Interp}}}{\mathrm{HTM1}_{\mathrm{Exp}}} \cdot 100\%. \tag{3.2}$$

Some quantities are measured starting from 1 (stretch), so for calculating percent differences 1 is subtracted from denumerator

$$\mathrm{TZo1}_{\text{percent diff}}(\mathrm{Stretch}) = \frac{\mathrm{TZo1}_{\mathrm{Exp}} - \mathrm{TZo1}_{\mathrm{Interp}}}{\mathrm{TZo1}_{\mathrm{Exp}} - 1} \cdot 100\%. \tag{3.3}$$

## 3.6 Statistical Analysis

Having effective mechanical properties obtained with the tool developed in the previous section (section 3.5), the properties can be grouped and statistically analyzed. Statistics

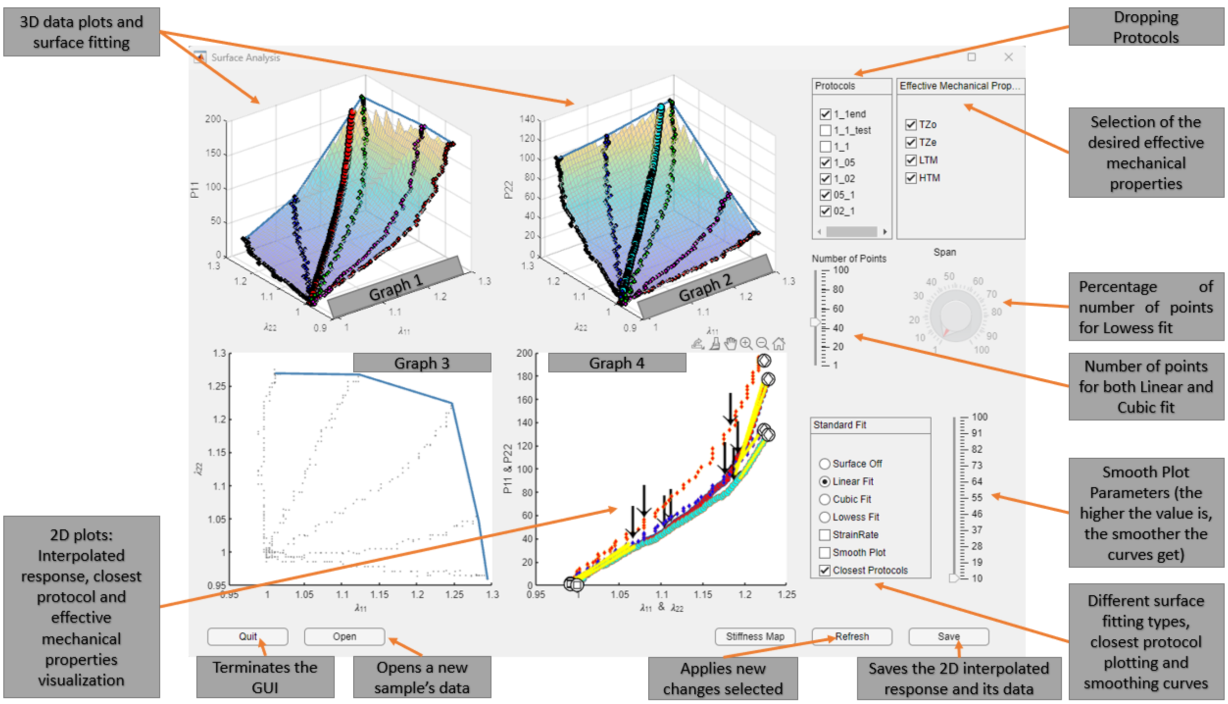


Figure 3.3: Example of a data set using the developed surface fitting program

can be used to assess how extraction methods affect the outcome of the study and how the mechanical properties associated with grouped specimens vary.

Mechanical properties are often non-normal, so to have a valid analysis, we considered the normality of these data and evaluated it using the Shapiro-Wilk test. Then, the comparison was assessed based on the number of groups. In the case of two groups, T-test was used for normal data, and the Mann-Whitney U test was applied to non-normal data. On the other hand, having three or more groups resulted in using the ANOVA test for normal data and the Kruskal-Wallis H test for non-normal data. This will help determine significant differences between selected groups via the evaluation of $p$-values. For instance, a $p$-value less than the predetermined significance level (e.g., $p = 0.05$) suggests a statistically significant difference, while a $p$-value higher than the significance level indicates no significant difference. In figures, asterisks "*" will be used to indicate significant differences, with a single "*" for $p \leq 0.05$, double "**" for $p \leq 0.01$, triple "***" for $p \leq 0.001$ and quadruple "****" for $p \leq 0.0001$.

Next, two additional parameters will be used in statistical discussions. First, the median $Q_2$: this parameter determines the central tendency, which is characterized by the middle value resulting from arranging each dataset in an increasing or decreasing order. After arranging a dataset, the median can be extracted or calculated: if the number of values in the dataset is odd, the median is exactly the middle value. Whereas, if the number of values is even, the median is the average of the two middle values. Then, the second parameter is called iQR. It is a statistical indicator evaluating the region of variability of a dataset. In that manner, if the data is widely spread, the iQR is known to be larger, while if the data is more concentrated, the iQR should be smaller.

All statistical simulations are implemented using MATLAB (version R2022b).

# Chapter 4

# Demonstration of Capabilities of the Proposed Biaixial Data Extraction Approach Using Previously Published Biaxial Data

## 4.1 Objective

In this chapter, the second objective proposed in Chapter 2 will be fulfilled. The main idea is to test whether the proposed advanced method of biaxial data extraction (based on surface fitting) generates data different from the data produced by conventional biaxial data analysis. For this purpose, the existing biaxial data from aortic tissue samples will be utilized. First, the source of data will be discussed. Then the brief details/specifics of the sample preparation/experimental protocol will be provided (more detailed steps can be found in Chapter 3). The developed GUI will be used to process all data and generate two sets of effective mechanical parameters for each sample - based on the interpolated and based on experimental data extraction approach. Next, various statistical tests will be performed by either assessing the differences between the experimental and interpolated response of each effective mechanical property or comparing results within aortic tissue groups. Finally, the implications of choosing either conventional or proposed methods for biaxial data analysis will be discussed. Some interesting results related to aortic tissue comparisons will be highlighted.

## 4.2 Methodology

### 4.2.1 Tissue/Data Sourcing

The Biological Tissue Mechanics Laboratory (PI: Elena Di Martino, University of Calgary) kindly provided biaxial data from three groups of aortic tissues for analysis. Two groups of tissues came from human ascending aortic aneurysms with different types of valves, normal tricuspid aortic valves (TAV) and abnormal bicuspid aortic valves (BAV) [1, 104]. Human aneurysm samples were collected from surgical repairs of male and female patients with a mean age of 61.58 years (standard deviation of 11.5 years) with aneurysms of mean diameter of 5.31 cm (standard deviation of 0.75 cm). The third group of specimens came from healthy PIG animals [110] collected at a slaughterhouse (6-month-old, Yorkshire breed, 250 lb). Overall, data from 10 TAV samples, 13 BAV samples, and 8 PIG samples were used.

### 4.2.2 Specimens Preparation

All specimen preparation steps mentioned in Chapter 3 were followed. All samples were frozen at $-80°C$ and then thawed before testing. Human aortic specimens TAV were squares with at least 8 mm per side with the median thickness of $Q_2 = 2.06$ mm reported ($iQR = 0.49$ mm) [1]. There was no information on thickness provided for BAV samples, but the square samples' sides were at least 10 mm per side [104]. Then, the PIG samples were also squares of 13 × 13 mm with a median thickness of 2.1 mm [110]. Four hooks per side were used for TAV and BAV samples, and two hooks per side were used for PIG samples. Five dots were drawn on the surfaces of all samples from three aortic tissue groups for deformation tracking.

### 4.2.3 Testing Protocol

The ElectroForce Systems planar biaxial device (see Chapter 3 figure 3.1a) with two load cells (22 N each) from TA instruments (Springfield, MO, USA) was used to test the aortic tissue samples. A 0.01-0.05N preload was applied to all specimens. Human samples TAV and BAV were tested with a quasi-static loading rate of 0.33 mm/s and pre-conditioning of 10 loading-unloading cycles. The displacements were applied to reach the maximum strain of $\varepsilon_{L_{ii}} = 60\%$. To explore responses to a variety of loading regimes, protocols "1:1", "1:0.5", "1:075", "0.5:1", and "0.75:1" were conducted [1].

PIG samples were tested with a quasi-static loading rate set so that each cycle length was 10 s. Preconditioning was set to 5 loading-unloading cycles with a maximum strain of $\varepsilon_{L_{ii}} = 80\%$. Protocols "1:1", "1:0.5", "1:0.2", "0.5:1", and "0.2:1" were conducted [110].

## 4.3 Results

In this section, the effective mechanical properties for each group of aortic tissue samples were extracted following both the conventional approach of data extraction (extracting from protocol "1:1" and denoted as "Exp" referring to "experimental response" as defined in Chapter 3 section 3.5) and the proposed advanced technique of data extraction (referred to as "interpolated response" and denoted as "Interp"). The developed GUI was utilized. The median and interquartile values for all effective mechanical properties for each aortic tissue group (TAV, BAV and PIG) are summarized in Table 4.1.

As stated in the objective section of the current chapter (Section 4.1), the main focus is to show that the different data extraction approaches result in different outcomes. To validate that, differences between the experimental response and the interpolated response will be thoroughly explored.

| Property/Group | | TAV | | BAV | | PIG | |
|---|---|---|---|---|---|---|---|
| | | Exp | Interp | Exp | Interp | Exp | Interp |
| **TZo1-Stretch** | $Q_2$ | 1.094 | 1.087 | 1.075 | 1.065 | 1.1902 | 1.095 |
| | $iQR$ | 0.068 | 0.04 | 0.068 | 0.037 | 0.056 | 0.029 |
| **TZo2-Stretch** | $Q_2$ | 1.092 | 1.088 | 1.075 | 1.068 | 1.1902 | 1.095 |
| | $iQR$ | 0.063 | 0.029 | 0.071 | 0.04 | 0.058 | 0.034 |
| **TZo1:2-Stretch** | $Q_2$ | 1 | 1 | 1 | 1 | 1 | 1.001 |
| | $iQR$ | 0.0037 | 0.041 | 0.0057 | 0.0051 | 0 | 0.0048 |
| **TZo1-Stress (KPa)** | $Q_2$ | 17.65 | 16.18 | 23.49 | 25.29 | 42.69 | 32.8 |
| | $iQR$ | 13.96 | 12.07 | 15.86 | 15.12 | 7.74 | 5.9 |
| **TZo2-Stress (KPa)** | $Q_2$ | 15.54 | 15.39 | 22.09 | 24.37 | 36.59 | 21.84 |
| | $iQR$ | 11.39 | 11.96 | 18.54 | 19.22 | 6.33 | 8.37 |
| **TZo1:2-Stress** | $Q_2$ | 1.078 | 1.039 | 1.021 | 1.084 | 1.058 | 1.65 |
| | $iQR$ | 0.403 | 0.58 | 0.39 | 0.54 | 0.19 | 0.51 |
| **TZe1-Stretch** | $Q_2$ | 1.182 | 1.148 | 1.163 | 1.123 | 1.361 | 1.176 |
| | $iQR$ | 0.097 | 0.053 | 0.081 | 0.07 | 0.078 | 0.047 |
| **TZe2-Stretch** | $Q_2$ | 1.181 | 1.151 | 1.166 | 1.123 | 1.365 | 1.186 |
| | $iQR$ | 0.123 | 0.06 | 0.083 | 0.058 | 0.085 | 0.055 |
| **TZe1:2-Stretch** | $Q_2$ | 1 | 1 | 1 | 1 | 0.997 | 1 |
| | $iQR$ | 0.00065 | 0.0069 | 0.00029 | 0.008 | 0.0057 | 0.0059 |
| **TZe1-Stress (KPa)** | $Q_2$ | 42.53 | 36.57 | 56.09 | 24.85 | 107 | 68.32 |
| | $iQR$ | 32.86 | 25.04 | 39.38 | 33.52 | 21.63 | 14.42 |
| **TZe2-Stress (KPa)** | $Q_2$ | 40.02 | 27.81 | 50.54 | 48.08 | 94.05 | 45.1 |
| | $iQR$ | 25.07 | 24.004 | 44.28 | 39.84 | 15.02 | 17.8 |

| | | | | | | | |
|---|---|---|---|---|---|---|---|
| **TZe1:2-Stress** | $Q_2$ | 1.086 | 1.039 | 1.032 | 1.078 | 1.06 | 1.65 |
| | $iQR$ | 0.44 | 0.603 | 0.42 | 0.53 | 0.21 | 0.48 |
| **LTM1 (KPa)** | $Q_2$ | 149 | 152 | 328 | 373 | 246 | 294 |
| | **iQR** | 125 | 128 | 108 | 165 | 41.2 | 87 |
| **LTM2 (KPa)** | $Q_2$ | 156 | 145 | 296 | 320 | 179 | 173 |
| | $iQR$ | 80.68 | 99.28 | 80.32 | 119 | 25.64 | 30.9 |
| **LTM1:2** | $Q_2$ | 1.106 | 1.079 | 1.105 | 1.133 | 1.307 | 1.59 |
| | $iQR$ | 1.12 | 0.93 | 0.39 | 0.31 | 0.42 | 0.52 |
| **HTM1 (KPa)** | $Q_2$ | 626 | 544 | 622 | 655 | 591 | 683 |
| | $iQR$ | 736 | 566 | 572 | 361 | 255 | 113 |
| **HTM2 (KPa)** | $Q_2$ | 553 | 420 | 594 | 678 | 591 | 438 |
| | $iQR$ | 678 | 854 | 816 | 481 | 272 | 287 |
| **HTM1:2** | $Q_2$ | 1.05 | 1.084 | 0.89 | 1.002 | 0.773 | 1.5 |
| | $iQR$ | 0.57 | 0.55 | 0.56 | 0.42 | 0.39 | 0.63 |

Table 4.1: Median and interquartile values of effective mechanical properties for TAV, BAV and PIG aortic tissue groups.

### 4.3.1 Influence of the Data Extraction Method on Parameters Within Each Group

First, we study how each effective mechanical property is affected by the extraction algorithm in each aortic tissue group. Figures 4.1, 4.2 and 4.3 show the boxplots of all effective mechanical properties derived by two extraction methods ("Interp" and "Exp") plotted for TAV, BAV and PIG groups.

Starting with effective mechanical properties characterizing the onset of the transition zone for human samples, TZo-Stretch/Stress values derived by the conventional extraction method ("Exp") were not significantly different ($p > 0.05$) from values obtained by the

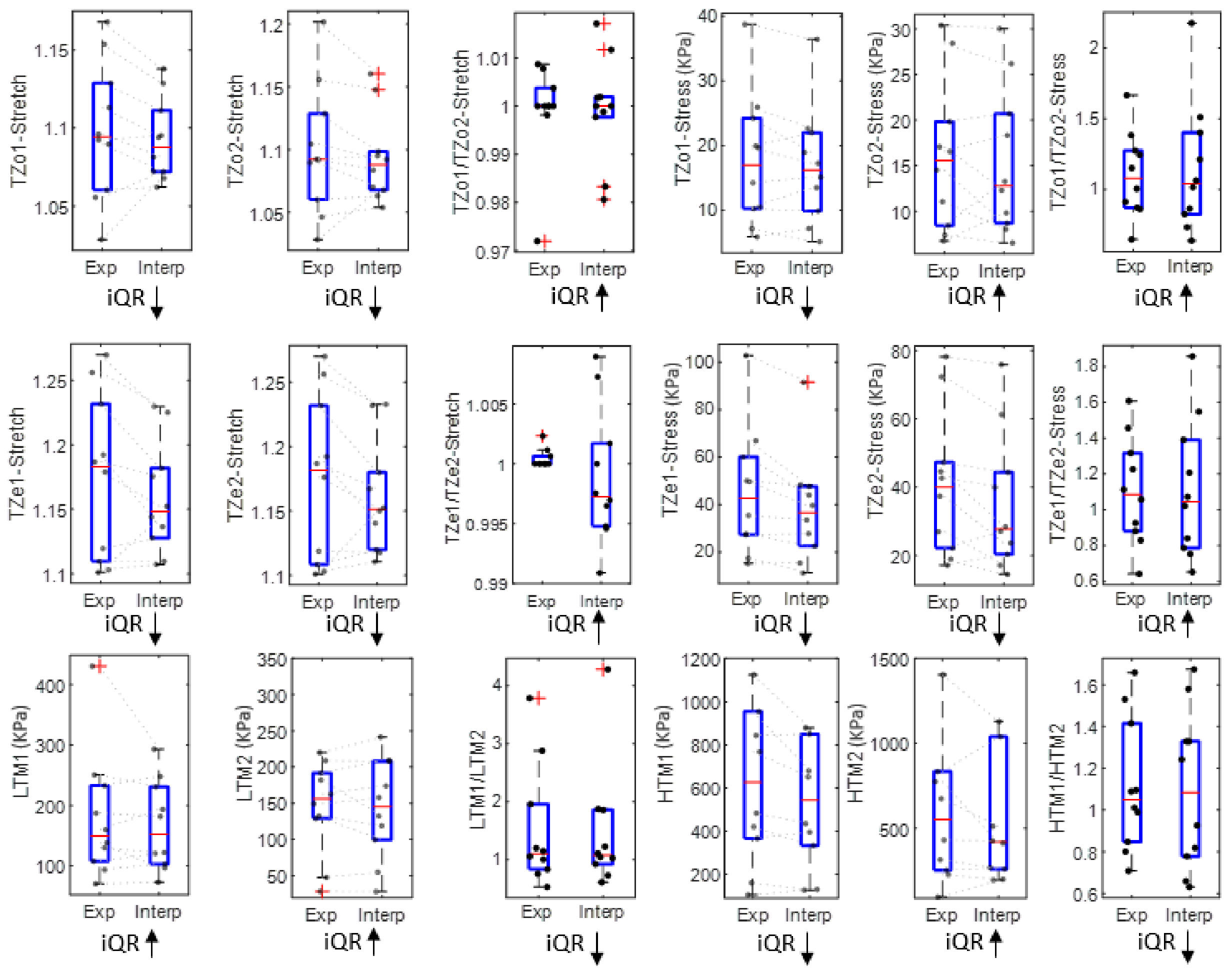


Figure 4.1: Effect of the data extraction approach ("Exp" and "Interp") on the effective mechanical properties within human aortic tissue group TAV.

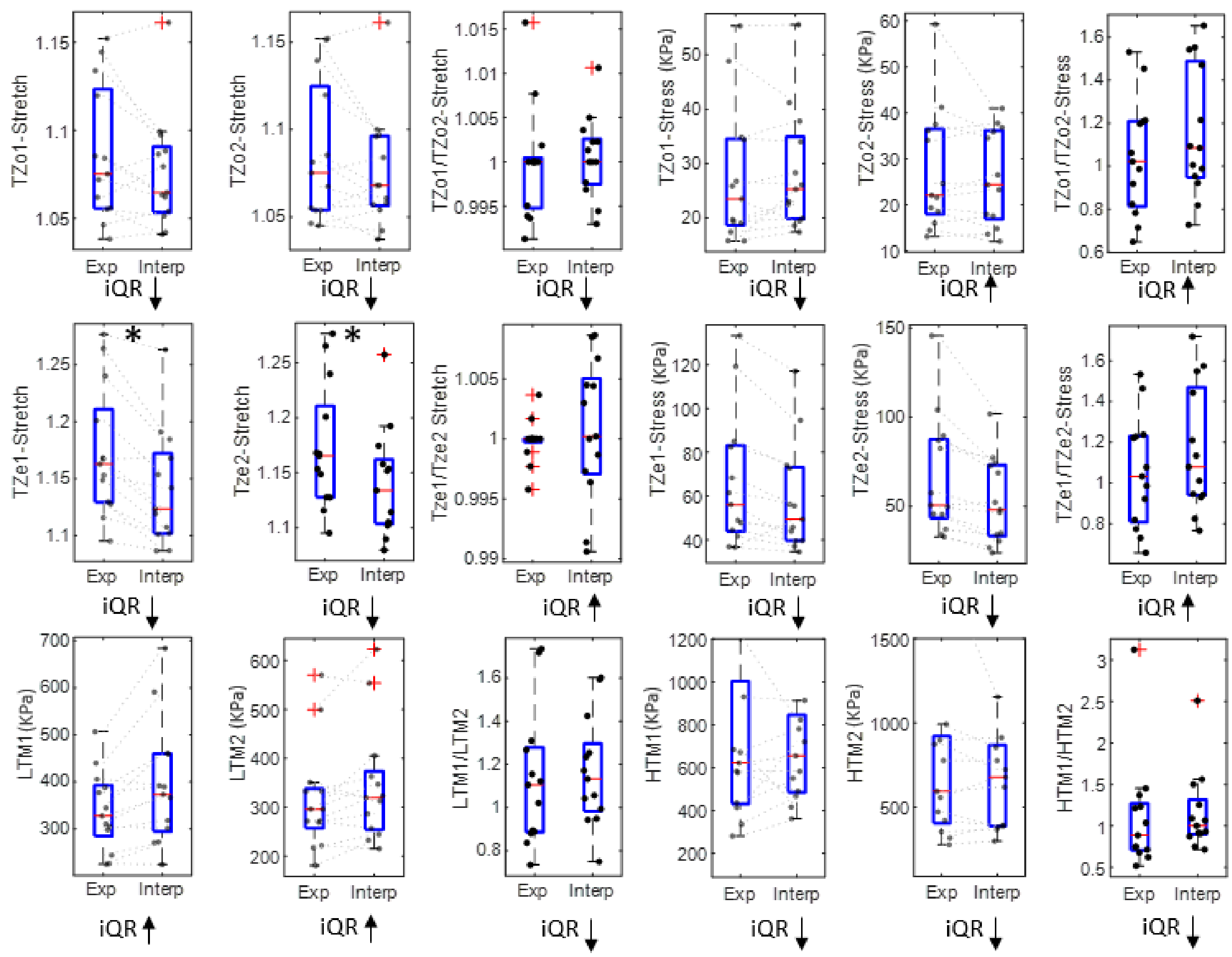

Figure 4.2: Effect of the data extraction approach ("Exp" and "Interp") on the effective mechanical properties within human aortic tissue group BAV.

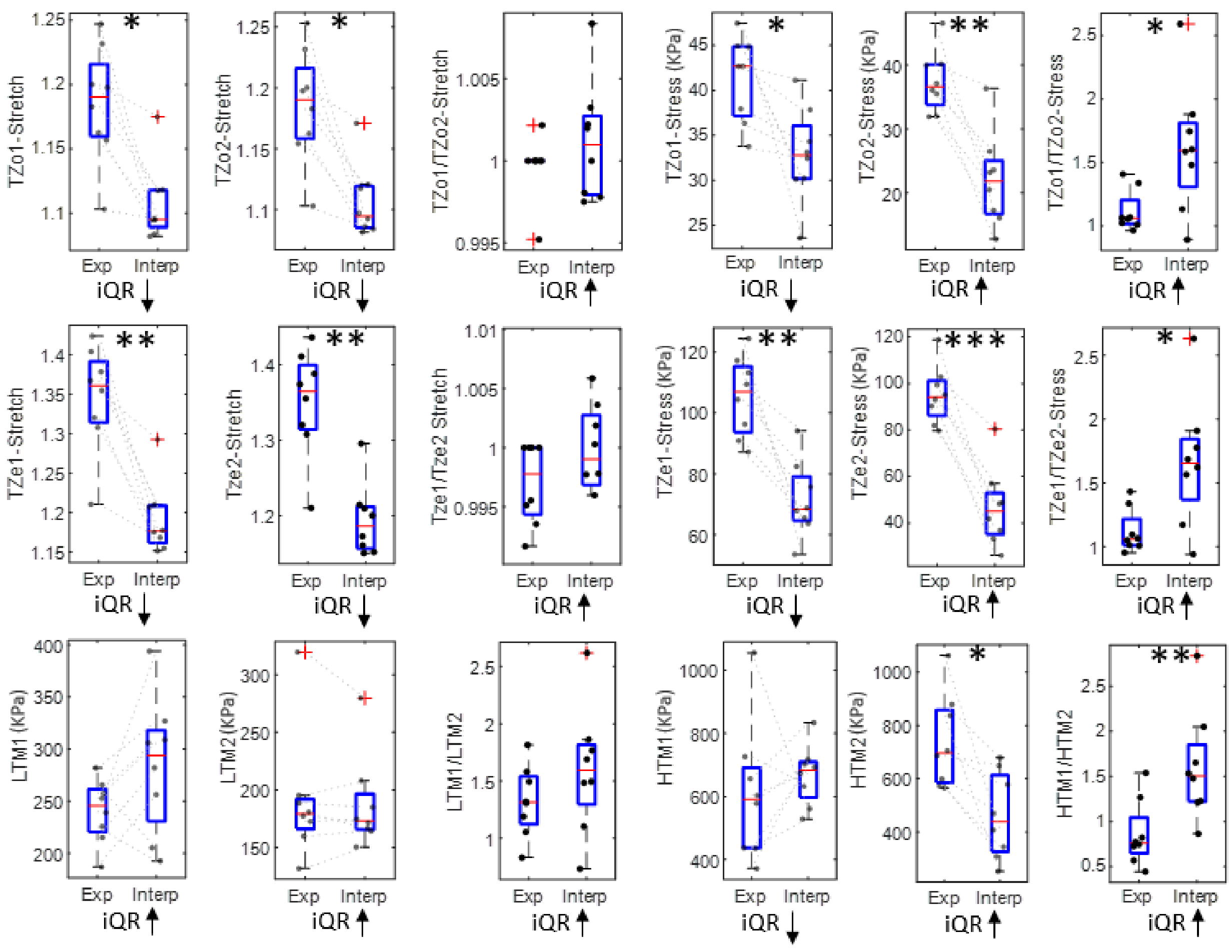


Figure 4.3: Effect of the data extraction approach ("Exp" and "Interp") on the effective mechanical properties within porcine aortic tissue group PIG.

advanced extraction approach ("Interp"). However, for TZo-Stretch, the variability in the data ($iQR$) was decreased for the "Interp" type of analysis as visualized in figures 4.1-4.2 and reported in table 4.1. As for the porcine aorta (PIG), the significant differences between "Interp" and "Exp" types of analysis were detected: 1) TZo-Stretch with $p$-values equal to 0.02 in both directions, 2) TZo-Stress with $p$-values equal to 0.02 and 0.003 in directions "11" and "22" respectively (see figure 4.3). As for the anisotropy ratios TZo1:2-Stretch and TZo1:2-Stress, the type of analysis ("Exp" and "Interp") had a mixed impact on the resulting properties. Extraction of data using the advanced approach ("Interp") made some properties more isotropic (e.g, TZo1:2-Stretch for BAV), others - more anisotropic (e.g, TZo1:2-Stretch for PIG), with the trend of increased data variability $iQR$. For stresses in PIG group, there was a significant difference between values of anisotropy depending on the data extraction approach ($p = 0.02$).

Moving onto the properties characterizing the end of the transition zone, TZe-Stretch and Stress, the results are very similar to the onset of the transition zone. However, this time, there are also statistically different results depending on the type of analysis ("Exp" and "Interp") in TZe-Stretch for BAV group of human tissues ($p = 0.04$ in both directions), while the statistically significant differences for porcine tissues (PIG) are more pronounced (TZe1-Stretch: $p = 0.03$; TZe2-Stretch and TZe1-Stress: $p = 0.003$; TZe2-Stress: $p = 0.00007$) with the exception of TZe1:2-Stress, in which significance is similar ($p = 0.02$).

Now, the aim is to evaluate the mechanical properties associated with the stiffness of the response at the start and the end of the stress deformation curves - LTM and HTM. "Interp" type of analysis always increased variability in LTM and had a mixed effect on the variability of the data in HTM sometimes producing less variable data (HTM1) and more variable data in other instances (HTM2 for both TAV and PIG). The only significant changes due to the type of analysis used were observed in HTM2 and HTM1:2 (as seen in figure 4.3 for PIG group (respective $p$-values are 0.04 and 0.01).

### 4.3.2 The Most Affected Parameters based on the Percentage Differences

In this section, the percentage differences in all effective mechanical properties due to the new type of analysis ("Interp") will be investigated to assess which properties are the most affected by inconsistencies in the deformation states ("Exp"). Importantly, if in half of the samples, one property increased due to the new type of analysis and, in the remaining samples, it decreased by the same amount. Qualitatively, the comparison of median values will reveal no difference between data extraction approaches, while individual changes will still occur. In contrast, percentage difference analysis will capture individual changes.

Figure 4.4 shows percentage differences in all effective mechanical properties for each tissue type (TAV, BAV, PIG). For clarity, measures are grouped by type - Stretch, Stress, and Stiffness.

Changes in stretches due to the new type of analysis ("Interp") are fairly large, ranging between 0% and 70%, with the most notable changes for porcine aortic tissues. Generally, stretches associated with the onset transition zone and the end of the transition zone are affected more, while anisotropy (TZo1/TZo2-Stretch and TZe1/TZe2-Stretch) is barely impacted.

Changes in stresses due to a new type of analysis are more noticeable with the median values ranging between 10% and 50%, qualitatively. In most tissue groups, the response in direction "22" is more affected than the response in "11" except for TZo2-Stress for BAV. As expected based on the previous section, a new type of analysis changed the data results for PIG tissue group the most.

Finally, changes in stiffnesses due to a new type of analysis ("Interp") are as noticeable as for stresses with a qualitative median ranging from 8% to approximately 20%. HTM was more affected than LTM for all groups but especialy for PIG. In contrast to stresses and stretches, the anisotropic ratio of stiffness values is quite impacted by the data extraction method ("Interp"), especially HTM for PIG reaching almost 200% as the highest

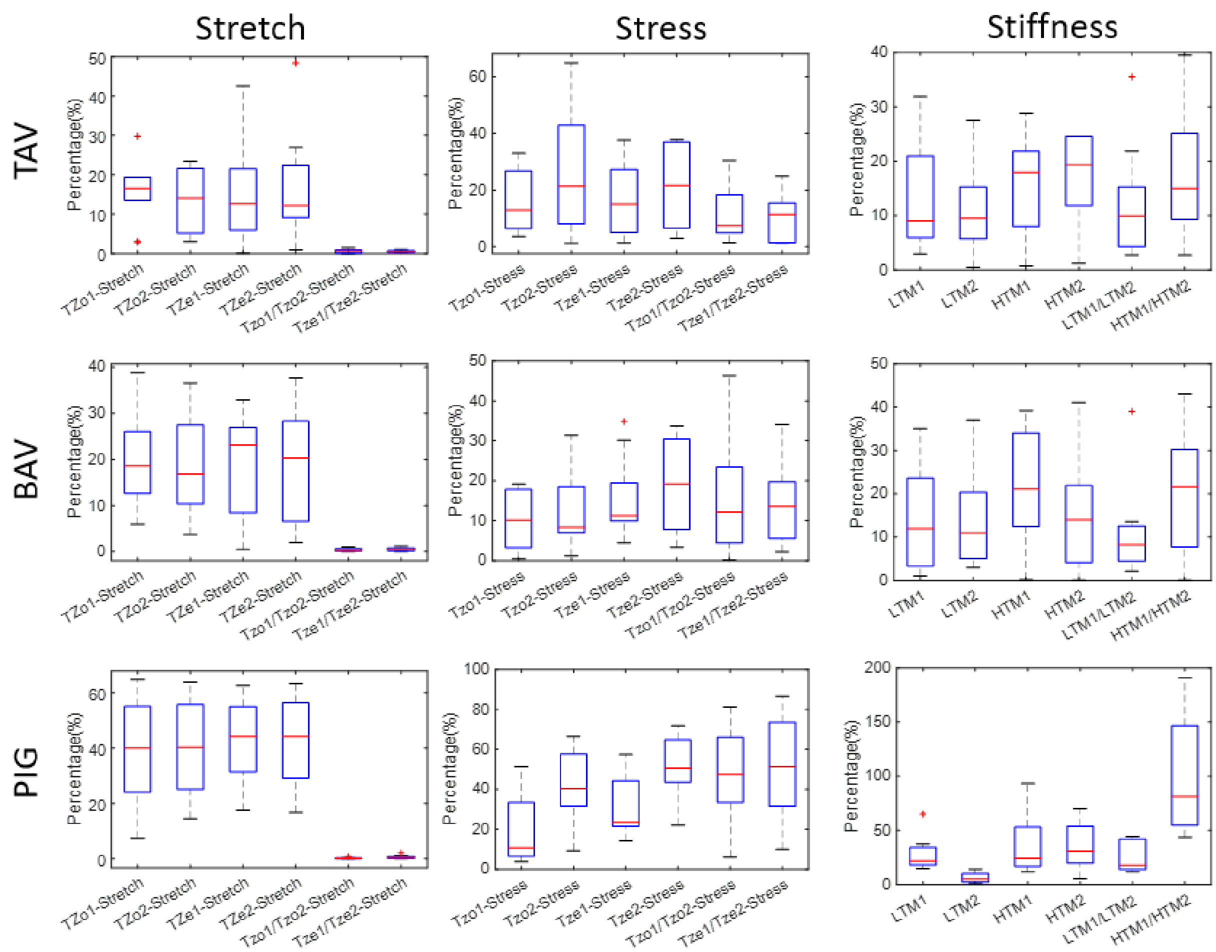


Figure 4.4: Percentage differences for all effective mechanical properties

percentage difference.

### 4.3.3 Influence of the Data Extraction Method on Comparison Within Groups of Interest

In this section, the goal is to compare the effective mechanical properties among the aortic tissue groups (TAV, BAV and PIG) and analyze how these groups differ. First, the statistical analysis will be done for the data extracted by the conventional approach at the different deformation states ("Exp"), then the process will be repeated for the data extracted from equivalent deformation states ("Interp"). We will assess if the data extraction process impacts group comparisons.

Figure 4.5 provides group comparisons for each property performed for "Exp" or "Interp" data separately. When TZo-Stretch and TZe-Stretch measures are obtained by "Exp" analysis, significant differences between aortic tissue groups are statistically detected (TZo1-Stretch: $p = 0.00004$, TZo2-Stretch: $p = 0.0001$, TZe1-Stretch and TZe2-Stretch: $p = 0.000001$). PIG samples seem to have a transition zone much later than human tissues. BAV have transition zone slightly earlier than TAV. However, when all measures are extracted at the equivalent deformation states ("Interp"), statistical significance with larger $p$-values compared to the "Exp" type of analysis (TZo1-Stretch: $p = 0.047$) or no significance at all (TZo2-Stretch: $p = 0.083$, TZe1-Stretch and TZe2-Stretch: $p = 0.05$) are observed. As for the anisotropy, the onset transition zone showed similar results for both types of analysis ("Exp" and "Interp"). All the properties (TZo1/TZo2-Stretch and TZe1/TZe2-Stretch) showed mostly an isotropic behaviour (see figure 4.5) except for PIG ("Exp") and TAV ("Interp") that had earlier full collagen engagement in the "22" direction. The significant differences between anisotropic stretch properties of different aortic tissue groups were only observed in TZe1/TZe2-Stretch extracted using the conventional approach ($p = 0.022$).

Next, figure 4.5 also depicts the same groups' comparison but for the stress properties.

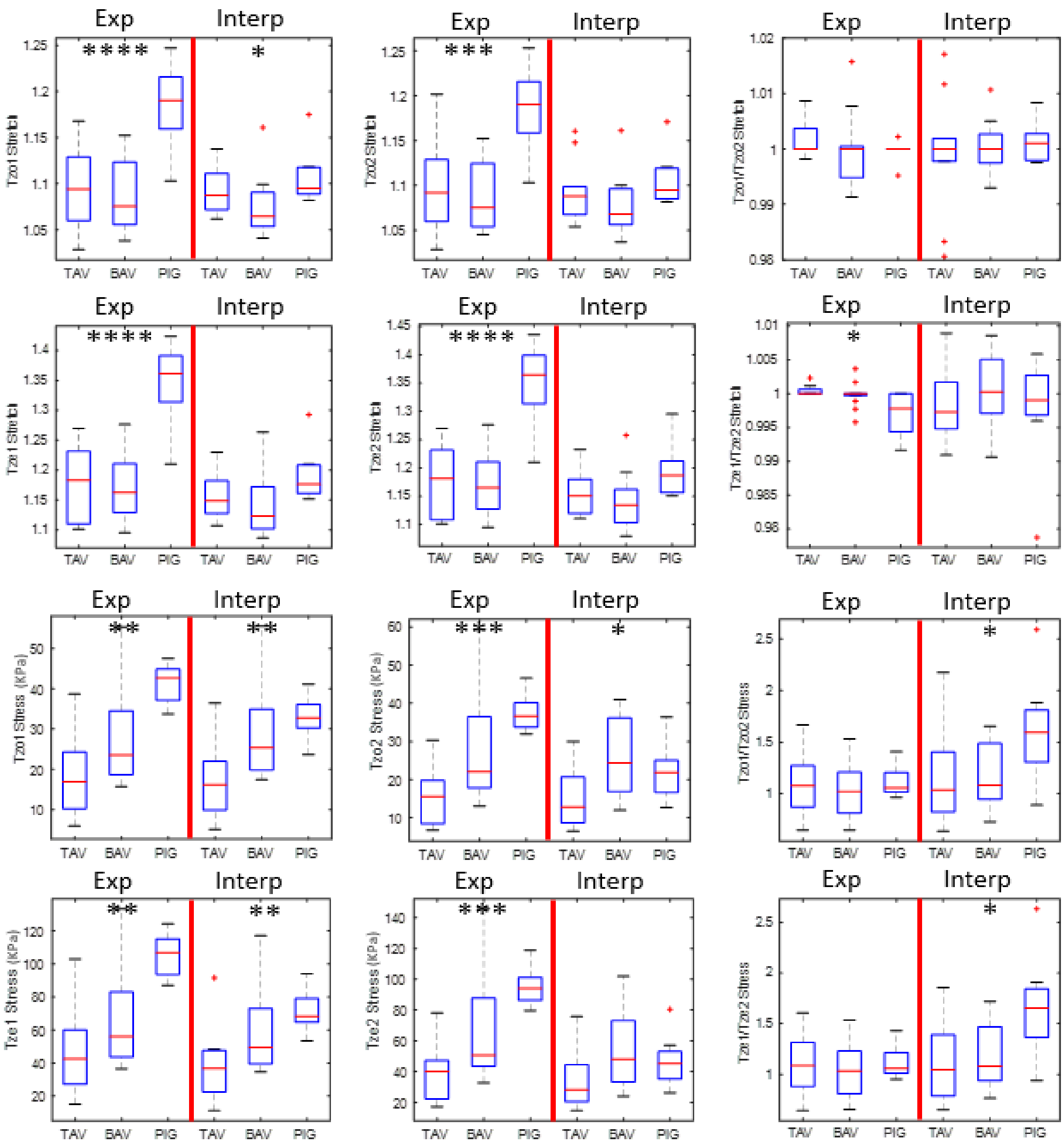

Figure 4.5: Effect of the data extraction approach on the stretches and stresses within the experimental groups and interpolated groups

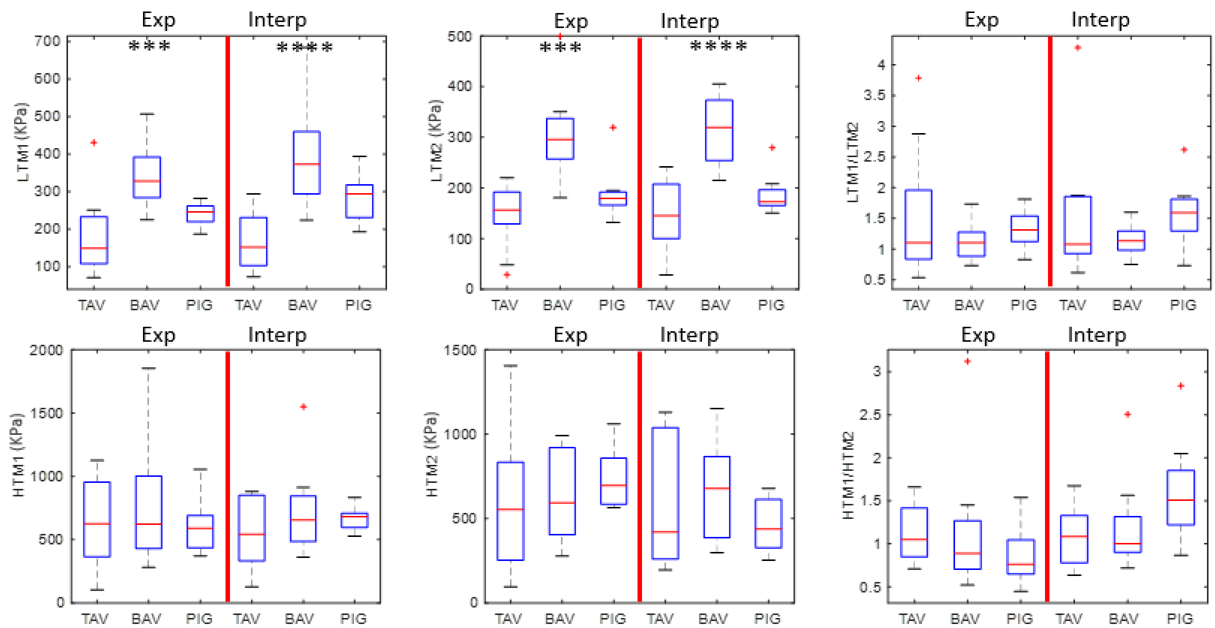


Figure 4.6: Effect of the data extraction approach on the stiffness within the experimental groups and interpolated groups

While the stretch properties discussed earlier in this section showed mixed results, the groups revealed a higher tendency towards significant differences for most stress properties using conventional and advanced approaches ("Exp" and "Interp"). Some of them showed some significant differences extracted using the conventional approach (TZo1-Stress and TZe1-Stress: $p = 0.001$), while others showed lower p-values indicating this significance (TZo2-Stress: $p = 0.0006$ and TZe2-Stress: $p = 0.0007$). As for the advanced approach, all the properties also showed significant differences mostly presenting higher p-values than for the conventional approach except for the end transition zone property in direction "22" ($p = 0.15$). While the stress properties mostly showed significant differences for all the properties extracted using both approaches ("Exp" and "Interp"), the ratios for each of the onset and end of the transition zone properties only showed significant differences for the data extracted using the advanced approach (TZo1/TZo2-Stress: $p = 0.04$ and

TZe1/TZe2-Stress: $p = 0.01$). Some interesting results can be reported for aortic tissues. By comparing the conventionally derived transition zone stresses, PIG tissues had the highest stress values followed by BAV and then TAV. However, both PIG and BAV showed mostly similar values using the advanced data extraction approach. Interestingly, PIG exhibits the highest anisotropy using the advanced approach, while this was not visible at all using the conventional data extraction approach.

Moving to the properties associated with stiffness, and as illustrated in figure 4.6, at the start of the stress deformation curves, LTM revealed significant differences for the extracted data both using the conventional approach and the advanced approach (LTM1-Exp: $p = 0.0004$, LTM2-Exp: $p = 0.0001$, LTM1-Interp: $p = 0.00006$ and LTM2-Interp: $p = 0.00004$). As for the end of the stress deformation curves, HTM showed contradicting results. None of the extracted data for high tangent moduli showed significant differences within the groups for both approaches (HTM1-Exp:$p = 0.9$, HTM2-Exp=$p = 0.5$, HTM1-Interp: $p = 0.57$ and HTM2-Interp: $p = 0.32$). Next, stiffness ratios computed for the anisotropy analysis did not show any significant differences ($p > 0.05$). Now, it is interestingly noticeable that BAV revealed the highest LTM in both the conventional and the advanced approach. However, HTM1 showed closer median values qualitatively for the three aortic tissues, but HTM2 values were varying. PIG appeared to have the highest HTM2 using the conventional approach, while, for the advanced approach, BAV was the stiffest. As for anisotropy, the type of analysis did not show any major impact, keeping PIG the most anisotropic. Now, switching to HTM, PIG showed anisotropy in both approaches where the ratios revealed that HTM1 was stiffer being extracted using the conventional approach compared to HTM2 which was higher using the advanced data extraction approach.

## 4.4 Discussion

The goal of the chapter was to demonstrate that the way the effective mechanical properties are extracted can have a significant impact on the outcome of the study.

First, we analyzed the impact of the extraction method on all effective parameters within individual aortic tissue groups. A lot of significant differences were observed, especially in PIG tissue where the transition zone parameters were affected the most. While human aortic tissues did not show major significant differences, the type of data extraction impacted the variability in effective mechanical properties ($iQR$), with, for instance, a decreasing variability in stretches that can potentially impact any statistical analysis that explores collagen recruitment through biaxial response.

To further investigate the impact of the type of analysis, we explored how conventionally derived individual effective mechanical properties change when the advanced type of data extraction is used. For this purpose, the percentage differences between "Exp" and "Interp" values were calculated. Nearly all effective parameters are affected by the median percentage changes due to the type of analysis ranging between 15% and 20% in all the groups, with even higher values in PIG aortic group.

Finally, we performed aortic tissue group comparisons to investigate how the statistical outcome is affected by the type of analysis. In some cases (i.e., stretches), the conventionally derived data revealed statistical differences with lower p-values between tissue groups. These differences were either revealed with higher p-values or just diminished when the advanced data extraction approach was used. In other cases (i.e., stresses), significant differences were observed using both approaches or using only the advanced extraction technique.

It is evident that the outcome of the data analysis is affected by the type of data extraction used. Because different deformation states trigger the tissues' load-bearing microstructure differently, the comparison between effective mechanical properties from samples with different deformation states might lead to false statistical outcomes. We believe that effective mechanical properties should be compared at the equivalent deformation states. Many studies urged to use the correctly extracted data, with some employing constitutive modelling [1, 43] and others using similar methods to ours [46, 111]. However, to the best of our knowledge, only this study investigated the exact effect of the extraction method and provided evidence of potential inaccuracies.

Speaking of aortic tissues, the analysis of the presented effective mechanical properties is very important in understanding the health and pathology of the aorta. As mentioned earlier, porcine aortic tissues were the most affected during this study and that is due to several factors. One of these reasons is the testing protocol. Higher strains were applied to porcine aortic tissues compared to human aortic tissues allowing to explore more extreme deformations. Furthermore, pig aortas came from breed/age/weight-matched animals, whereas the human aortas came from donors of different ages, sexes, aneurysm sizes, and likely different aneurysm progression stages. This could be another reason behind the affected statistical comparison and the increased variability observed in the results. Notably, different studies proved that pig aortic tissues can represent human aortic tissues in research, thus, porcine aortic tissues can be a healthy substitute for human tissues [112, 113].

Overall, we were able to capture some interesting differences between different aortic tissue groups. As introduced in Chapter 1, elastic fibres are responsible for the linear region at the start of the stress-deformation curves. Therefore, LTM associates with elastic fibres/ground substance behaviour. It was observed that LTM were the largest for BAV among the other aortic tissues. One would expect healthy PIG tissues to exhibit higher elasticity (ability to recoil) [112] because aneurysm progression in human tissues causes elastin to degrade. But in the context of this thesis, porcine aortic tissues came from descending aorta which is expected to be less elastic than tissues excised from ascending aorta.

As for the other effective mechanical properties, the collagen engagement patterns are characterized by the transition zone properties (see Chapter 1). Interestingly, stretches and stresses, illustrating the onset and end of the transition zone, were significantly, if not, the most affected. In pathology, elastic fibres are replaced by collagen leading to the importance of these parameters in tracking the progression of aneurysms [104]. Noticeably, and qualitatively, the overall higher median values were found for PIG compared to TAV and BAV. This proves that the collagen fibres engaged earlier in human aneurysmal tissues compared to porcine aortic tissues demonstrating the unhealthy behaviour of the collagen fibres replacing elastic fibres in pathology.

Both effective mechanical properties extraction techniques revealed different results emphasizing the fact that the choice of extraction method does matter. However, the literature on modelling biaxial testing conditions (such as biaxial sample attachment, load application and etc.) aimed to improve/standardize the biaxial testing experiment highlighting the importance of measuring the deformations at the center of the specimens to diminish the boundary effects at the edges [114–117]. These studies further insist that the load applied at the borders of specimens in soft biological tissues does not transfer to the middle of the specimens in the same way due to differences in the specimens' microstructure. Therefore, identical experimental conditions at the boundary (which are also hard to ensure for two different specimens due to size/difference and hooks/rakes placement) will lead to different experimental loading conditions at the center of the specimens. As such, it is undoubtedly better from the general mechanical point of view as well as based on the bulk of the literature modelling the biaxial experiment to compare tissue response readings at equivalent loading conditions at the center of the specimens, which are only obtained through approaches like ours. Therefore, our data extraction approach is better while the commonly used data extraction approach based on protocol "1:1" can lead to inconsistencies and inaccuracies in the data as demonstrated in section 3.4 for aortic tissue groups specifically. Nevertheless, future research can evaluate whether the effect of the consistent data extraction approach (equivalent loading conditions at the border vs. equivalent loading conditions at the center of specimens) is critical enough for specific tissue groups to be worth integrating as an additional step in data analysis.

## 4.5 Limitations

Some limitations were encountered which could have an impact on the results observed in the current chapter. First, as seen in section 4.2.2, the human aortic specimens (BAV and TAV) were cut into squares having different sizes compared to the samples of the porcine aorta, as well as fewer number of samples available were for PIG. Moreover, although the human aortic tissues are comparable to porcine aortas [112], in this chapter, the collected data came from different locations within the aorta: from the ascending aorta for humans and the descending aorta for pigs. Ideally, it would be more reliable if healthy human aortic tissues were available instead of healthy porcine tissues. Next, aneurysmal tissues belonged to patients of different ages and stages of aneurysm progression which impacted the statistics as well. Also, due to the limited availability of soft tissues, this study only relied on these three aortic tissues, but we do believe that the evaluation of the impact of the extraction method in additional types of tissues would be very beneficial. Finally, it should be noted that the aortic tissue group comparisons would benefit from additional post hoc analysis to make a more specific conclusion on group differences but it was out of the scope of this chapter, where the focus was on the extraction method comparisons.

# Chapter 5

# Capabilities of the Proposed Biaxial Data Extraction Approach to Study Effects of Freezing and Heterogeneity on Skin Biomechanics

## 5.1 Objective

In this chapter, the aim is to apply the new advanced data extraction approach to study the effects of freezing and heterogeneity in the human back skin following the third objective proposed in Chapter 2. First, we will discuss where the tissue came from and how it was stored and tested. Next, similarly to the previous chapter (Chapter 4), two approaches of biaxial data extraction will be applied for data analysis. Along with demonstrating the different outcomes of different types of analysis, the effect of freezing and heterogeneity will be statistically evaluated. First, we will discuss if there is a difference in skin biomechanics depending on the freezing protocol. Then, we will assess whether effective mechanical properties vary across the different locations on the human's back.

## 5.2 Methodology

### 5.2.1 Specimens Collection

The study was approved by the University of Waterloo's Office of Research Ethics (Title: Effect of Freezing and Anatomic Location on Skin Mechanical Properties; Application No. 44749). Forty-two skin samples were collected from a 88 years old human male donor after an autopsy at the School of Anatomy (Kinesiology and Health Sciences Department, University of Waterloo, Waterloo, Canada) after approval from the Office of the Chief Coroner and the Ontario Forensic Pathology Service. These samples were excised from the donor's back and then divided into four groups of fourteen specimens. Figure 5.1 illustrates the donor's back divided into sets of two symmetric columns separated by the spine (red line). The aforementioned forty-two samples were divided equally on each of the left (denoted as "L") and right (denoted as "R") sides of the spine where the closest column to the spine is enumerated as column "1". For instance, a sample located in the left column close to the spine is labelled as "L1", and a sample located also on the left side but further from the spine is labelled as "L2". The orientation of the sample "11" and "22" are shown as perpendicular to the spine and parallel to the spine, respectively (see figure 5.1).

The orientation of each sample was marked on its top right corner, and every group of fourteen samples was immersed in three different solutions: 1XPBS ("FR"), Glycerol ("GL") and Liquid Nitrogen ("NG"). The pilot samples ("PL") were designated for trials. The choice of these freezing solutions was made based on several factors. For instance, PBS (Phosphate Buffered Saline) is commonly used in studies either as a thawing procedure after the freezing of soft tissues [118] or a hydration technique before freezing or even as a freezing protocol [119]. Furthermore, Glycerol also made its way in the freezing studies [120] as it has a decreased soft tissue cell toxicity [121], can spread through the cells and it can provide stability to the cell membrane [122]. Interestingly, some studies revealed the solution used is a mix of PBS and Glycerol where 10% of Glycerol is added to

PBS [123]. Indeed, Glycerol is considered a better way of freezing storage compared to PBS [124]. Therefore, it was intriguing to explore the biomechanical differences between these two storage protocols. Additionally, the effect of Liquid Nitrogen, commonly used for rapid dry tissue freezing, on skin biomechanics was of interest here since such freezing protocol is known to cause ice crystal formation and tissue cell death [125]. In the case of Liquid Nitrogen, no PBS was added to the tissue so it was a dry environment. After the preparation required for the specific freezing solutions, each sample was enclosed in a small container. After that, the containers were transported to the lab on ice in a tightly locked large container following the University of Waterloo regulations and transferred to a freezer at $-80°C$.

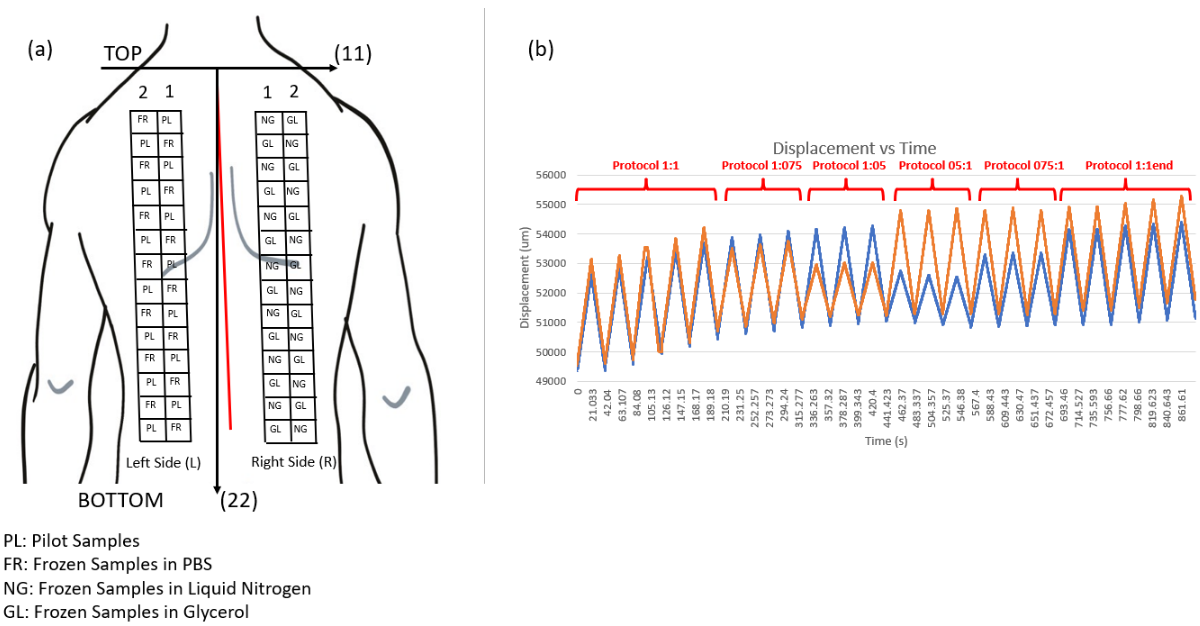


Figure 5.1: (a) Human donor back sketch showing samples' location. (b) Graph an example representing all the applied protocols with their number of cycles and applied displacement over time.

### 5.2.2 Samples Preparation

After storage for eight weeks, one sample at a time was taken out of the freezer and was thawed in PBS for fifteen minutes before testing. Following the sample preparation steps described in Chapter 3, each specimen was cut into a square of approximately 17 millimetres per side, and the subcutaneous fat was pulled out. The thickness for these specific tissue samples ranged between 1.9 to 2.5mm. Hooks were attached to the specimen, speckles were applied, and the sample was mounted to the CellScale Biotester 5000 machine to start the tests.

### 5.2.3 Testing Protocol

A preload of 40mN was applied and the camera frequency was set to 15 Hz. Then, each specimen was subject to five protocols at a maximum displacement equivalent to a 30% strain of the measured hook-to-hook distance at a strain rate equal to 1.5%/s, and the same 40mN preload was applied at the start of each cycle. The first protocol "1:1" consists of four preconditioning cycles and each of the remaining experimental protocols ("1:075", "1:05", "05:1" and "075:1") consisted of three cycles, with a standardized duration of forty seconds per cycle (see figure 5.1 (b)).

## 5.3 Results

In this section, we will first focus on the effect of freezing by conducting freezing protocols (PBS, Glycerol and Liquid Nitrogen) group comparisons for all the effective mechanical properties, extracted using both the conventional approach (referred to as "Exp") and the advanced approach (referred to as "Interp"). Next, we will move onto the discussion of skin heterogeneity by, first, displaying the effective mechanical properties along the back from top to bottom and, second, by grouping and comparing specimens based on their location w.r.t to the spine. As before, the process will be repeated for both types of extraction approaches.

### 5.3.1 Effect of Freezing by Comparing Effects of Different Storage Methods

In this section, the aim is to compare the effective mechanical properties of the tested human skin among three groups of specimens stored using freezing protocols: "PBS", "Glycerol" and "Liquid Nitrogen". The statistical analysis will be performed on the data extracted using the conventional approach ("Exp") and the advanced approach ("Interp"). The impact of each freezing solution will be assessed on the data extracted based on both approaches.

Figure 5.2 provides freezing protocol comparisons for all the effective mechanical properties associated with the transition zone (TZ-Stretch/Stress), for both "Exp" and "Interp" types of analysis. Irrespective of the type of analysis, for stretches and stretch ratios (anisotropy), there is no difference between different freezing protocols and the overall behaviour is fairly isotropic. Now, regarding the freezing protocol, it is visible that, in most cases, the median values for the stretches were slightly higher for the Glycerol group of specimens than for PBS and Liquid Nitrogen groups, irrespective of the data extraction approach. Only TZe1-Stretch and TZe2-Stretch extracted using the "Exp" approach showed a similar median value for both PBS and Glycerol ($Q_2 \approx 1.06$), and these properties were slightly lower for Liquid Nitrogen ($Q_2 \approx 1.05$).

Moving to stresses, when TZo1-Stress and TZe2-Stress measures were obtained from the conventional approach, no significant differences were determined. Only the onset and end transition zones properties in direction "22" extracted using the "Exp" analysis revealed significant differences ( TZo2-Stress: $p = 0.03$ and TZe2-Stress: $p = 0.044$ ). However, these significant differences were not detected when using the "Interp" type of data extraction and considering equivalent deformation states. While some of the stress properties

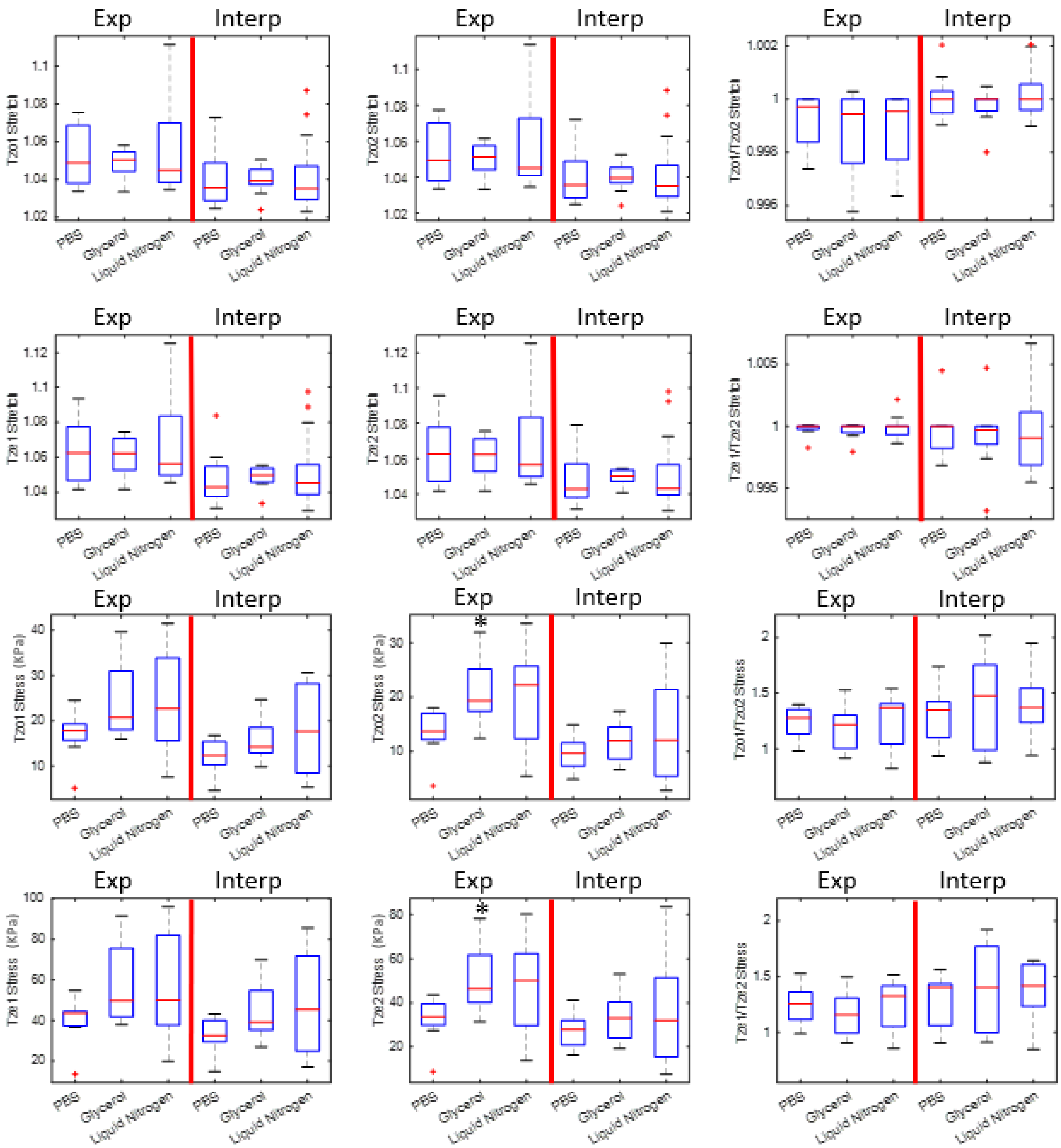


Figure 5.2: Effects of each freezing solution on the stretches and stresses extracted using the conventional and the advanced approaches

showed some significant differences, the onset and end stress transition zone ratios did not show significant differences at all for both extraction methods. Still, interesting results assessing the anisotropy were revealed. As shown in figure 5.2, the Liquid Nitrogen properties, extracted using both the “Exp” and “Interp” type of analysis, showed a more anisotropic behaviour. Interestingly, Liquid Nitrogen measured the highest median values, qualitatively, for the onset transition zone stresses among all the other groups ($Q_2 \approx 25$ KPa) for the data extracted using the conventional approach. While TZo1-Stress also showed the highest median for Liquid Nitrogen using the “Interp” analysis ($Q_2 \approx 18$ KPa), the end transition zone stress property in direction “22” had almost equal medians for both Glycerol and Liquid Nitrogen. Similar results were observed for TZe1-Stress and TZe2-Stress where the highest median values were recorded qualitatively for Liquid Nitrogen for TZe1-Stress extracted using the advanced approach and TZe2 extracted using the conventional approach. Overall, the lowest stress properties' values were revealed in PBS group for both the onset and the end transition zone properties.

Next, figure 5.3 depicts the effective mechanical properties associated with stiffness at the beginning and at the end of the stress-deformation curve. Starting with LTM, no significant differences were revealed for any of the data extracted through the “Exp” and “Interp” approaches. Similarly, HTM did not reveal significant differences for the data extracted using the conventional approach. However, the advanced approach showed a significant difference for HTM1 ($p = 0.049$). As for the anisotropy, none of the ratios showed any significant differences. “Interp” type of analysis displayed values with more anisotropic behaviour (e.g, HTM1/HTM2) or switched the stiffer direction (e.g, LTM1/LTM2). Furthermore, a qualitative assessment of the median values was performed on the stiffness properties. For for LTM, the median values showed mixed results. While LTM1 appeared to be the highest for Glycerol data extracted using the conventional approach, it switched to be the lowest using the advanced approach although a close value for Glycerol was maintained in both cases (PBS and Liquid Nitrogen groups went either lower or higher). As for HTM1, the highest median value was recorded for Liquid Nitrogen specimens using both the “Exp” and “Interp” approaches. While HTM2 also revealed the highest value using the

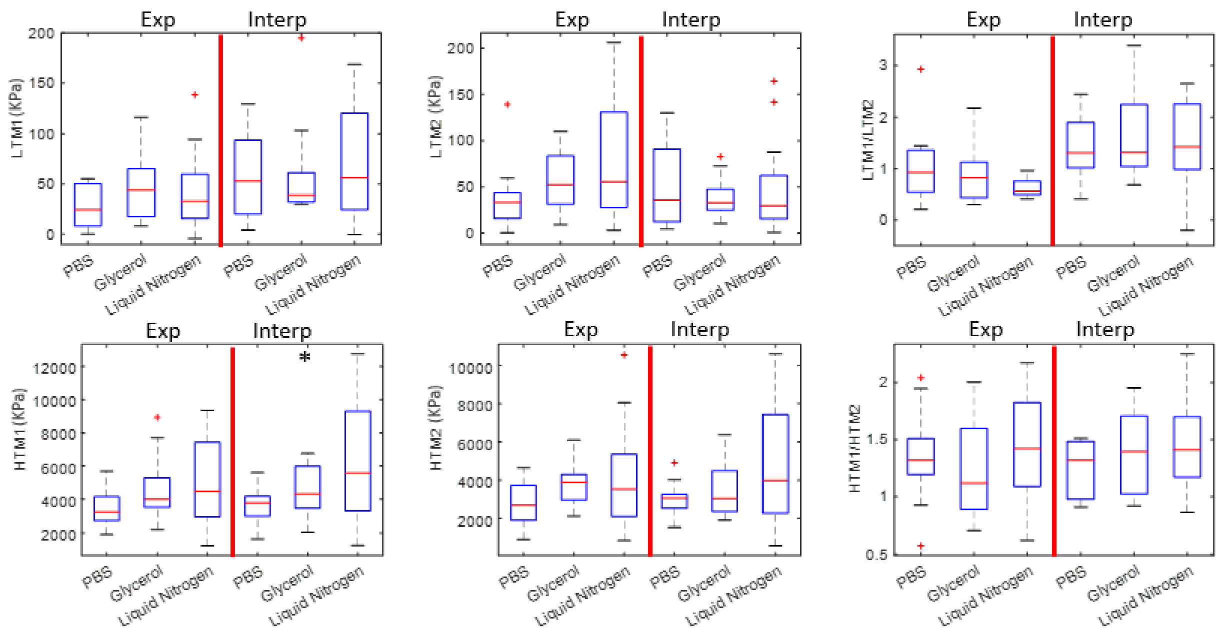


Figure 5.3: Effects of each freezing solution on the stiffness extracted using the conventional and the advanced approaches

“Interp” analysis for Liquid Nitrogen, this was not the case for the data extracted using the “Exp” approach where the Glycerol group was the stiffest.

### 5.3.2 Effects of Heterogeneity

In this section, we focus on investigating the heterogeneity across the human donor’s back based on the effective mechanical properties extracted using both the conventional approach (“Exp”) and the new type of analysis (Interp”). By plotting and analyzing these properties w.r.t their anatomic location (parallel and perpendicular to the spine) for each freezing solution used during the biaxial testing procedure, we gain insights into their variations across different regions of the skin. This approach enables us to visualize and assess how the mechanical properties differ depending on the location of the skin, thus proving

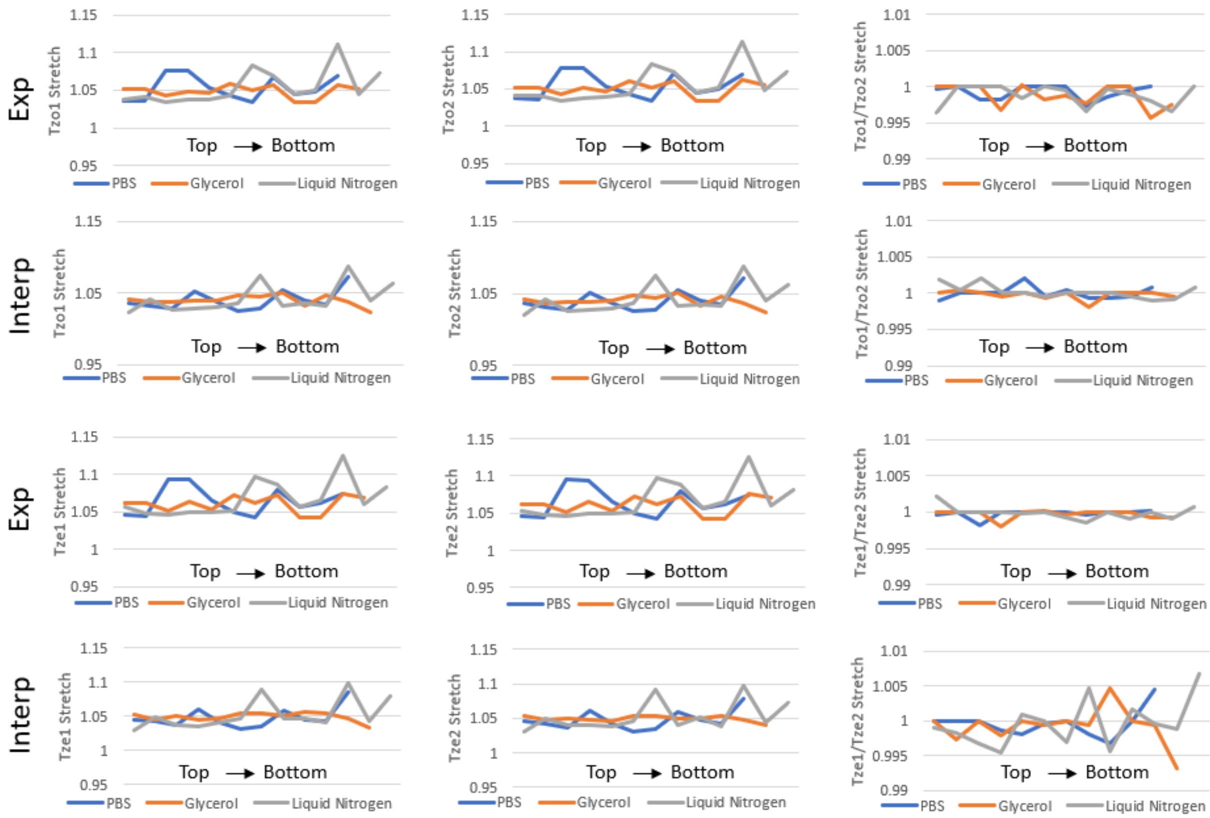


Figure 5.4: Transition zone stretch effective mechanical properties for each of the three freezing solutions

the heterogeneity in the skin's behaviour. Symmetry was assumed between the two left ("L") and right ("R") sides as supported by some studies [126].

Figure 5.4 reveals line plots displaying the TZ effective mechanical properties of the tested specimens with respect to their anatomic location along the back from the top to the bottom (Figure 5.1(a)). Different freezing protocols are outlined in different colours. Starting with transition stretches, some variability can be detected depending on the anatomic location with the highest TZo/TZe-Stretches observed in the Liquid Nitrogen group closer to the bottom of the back. However, the Glycerol group exhibits less variability especially


Figure 5.5: Transition zone stress effective mechanical properties for each of the three freezing solutions

when the "Interp" type of analysis is used. Noticeably, the onset and end of the transition zone stretch (TZo-Stretch and TZe-Stretch) recorded the highest value at the top of the back for the PBS data extracted using the "Exp" type of analysis. As for the anisotropy, mixed results were observed. First, the onset transition stretch exhibits higher values in direction "22" for the "Exp" type of analysis where the highest ratio reached did not exceed the value of 1. However, the data extracted using the "Interp" type of analysis revealed a more isotropic behaviour (closer to the value of 1) while having larger measures in the direction "11" at the top of the back. Similarly, the end transition zone stretches displayed an isotropic behaviour for the data extracted using the conventional approach ("Exp"),

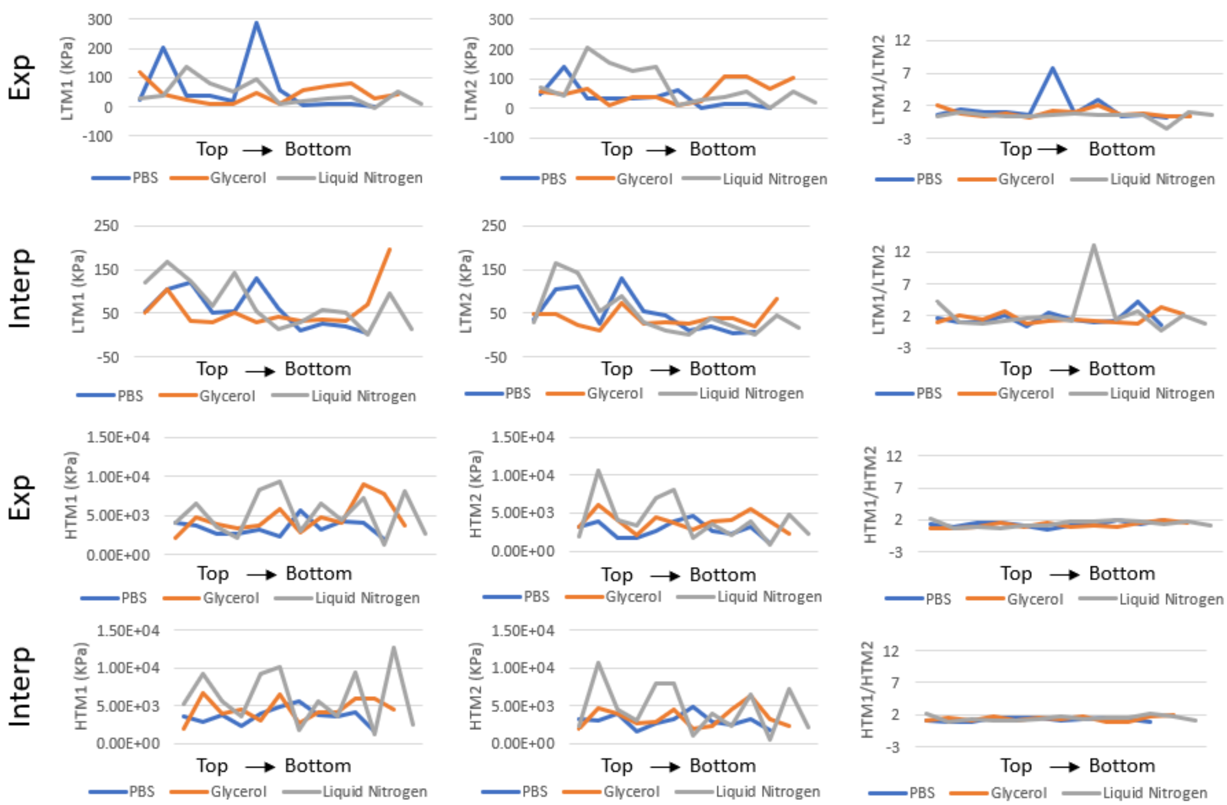


Figure 5.6: Stiffness effective mechanical properties for each of the three freezing solutions

where TZe1-Stretch was stiffer for Liquid Nitrogen and TZe2-Stretch was the stiffest for PBS and Glycerol groups at the top of the back. In contrast, the same properties extracted using the advanced approach ("Interp") revealed a lot of changes in the values where the stretch ratios seemed to either increase or decrease while going from the top of the back to the bottom.

In figure 5.5, both the onset and the end transition zone stresses are reported. Interestingly, these effective mechanical properties showed a more pronounced variability compared to the stretches, except for the PBS group. While PBS revealed the lowest values in all the properties for both the "Exp" and the "Interp" type of analysis, Glycerol and Liquid Nitrogen exhibited similar variations through the data extracted using the conventional approach ("Exp") where, most of the times, Liquid Nitrogen always had the tendency of higher stresses at the top of the back. Furthermore, samples stored using this freezing protocol exhibited a lot of jumps in stresses along the back. Moving to the bottom of the back, Glycerol samples had higher stresses compared to the other freezing protocols. However, the properties extracted using the "Interp" type of analysis revealed that the Liquid Nitrogen group displayed the highest values for both the onset and transition zone stresses. In that case, stresses showed some different results compared to stretches. Using the "Exp" type of analysis, the onset transition zone stress properties showed less variation than the end transition zone stress properties. Also, all transition stresses were fairly anisotropic with TZo and TZe stiffer in the "11" direction for most of the samples going from the top to the bottom of the back. Interestingly, the Glycerol group, most of the time, had the highest values for TZe1/TZe2-Stress for the data extracted using the conventional approach ("Exp").

Next, figure 5.6 shows the variations in stiffness properties along the back (lower and higher tangent moduli). Overall, the properties revealed a lot of jumps and variations. Strikingly, samples stored with Liquid Nitrogen exhibited the highest values for each of LTM2, HTM1 and HTM2 extracted using the "Exp" type of analysis at the top of the back. However, in this same location, LTM1 was the most pronounced for the PBS group. On the other side, at the bottom of the back, the Glycerol group made its way being the stiffest followed by the Liquid Nitrogen group. Although PBS specimens were showing larger stiffness values close to the other freezing protocols at the top of the back, for the samples located at the bottom of the back, the values were decreased. As for the data extracted using the advanced approach ("Interp"), the properties of the Liquid Nitrogen group were the stiffest at the top of the back, while Glycerol specimens had the lowest stiffnesses LTM1 and LTM2, and PBS group had lower values of HTM1 and HTM2. Interestingly, Liquid Nitrogen samples kept being stiff even at the bottom of the back for HTM1 and HTM2. However, in the same location, Glycerol was stiffer for the effective mechanical properties at the start of the stress-deformation curve (LTM1 and LTM2). As for anisotropy, LTM1/LTM2 revealed small variations for both the "Exp" and "Interp" types of analysis, except around the middle of the back, where the stiffness ratios reached peak values for the PBS group ("Exp") and for Liquid Nitrogen group ("Interp"). Same as for stresses, all the stiffness properties displayed anisotropic behaviour. Interestingly, LTM1/LTM2 exhibited very high values where the ratio exceeded 7 for PBS for the data extracted using the "Exp" type of analysis. Additionally, this same ratio almost reached a value of 14 for Liquid Nitrogen using the "Interp" type of analysis. As for the high tangent moduli ratio, both the data extracted using the conventional ("Exp") and the advanced ("Interp") approaches showed values hovering around 1.5 to 2, which confirms the anisotropy for these properties, as well as the fact that HTM1 was stiffer than HTM2 in both types of analysis.

Because a lot of jumps along the back were observed in the previous results of this section, an additional analysis was performed to study the results of taking samples from two locations with reference to the spine - close to the spine (e.g.: "L1") and further away from the spine (e.g.: "L2"). The specimens from each freezing protocol were grouped having a total of three sets of analysis. To better understand this procedure, and following the sketch in figure 5.1(a), the PBS samples are located on the left and divided into both columns "L1" and "L2".In contrast, the Glycerol and Liquid Nitrogen samples are located on the right side and divided into "R1" and "R2". Therefore, the PBS samples located in "L1" were compared to the PBS specimens located in "L2", and the same goes for the other freezing protocols where the samples in "R1" were compared to the samples of the same freezing solution in "R2". Due to the abundance of results, only the Liquid Nitrogen group was selected and discussed in this section, while the results for PBS and Glycerol groups were moved to Appendix A.

Figure 5.7 depicts the effective mechanical properties associated with the transition zone (TZ-Stretch/Stress), for both "Exp" and "Interp" types of analysis, comparing the samples of Liquid Nitrogen (NG) located in "R1" zone to the samples of Liquid Nitrogen (NG) located in "R2" zone (see figure 5.1(a)). Irrespective of the analysis type, the onset and end transition zone stretches in the sample group closer to the spine are significantly

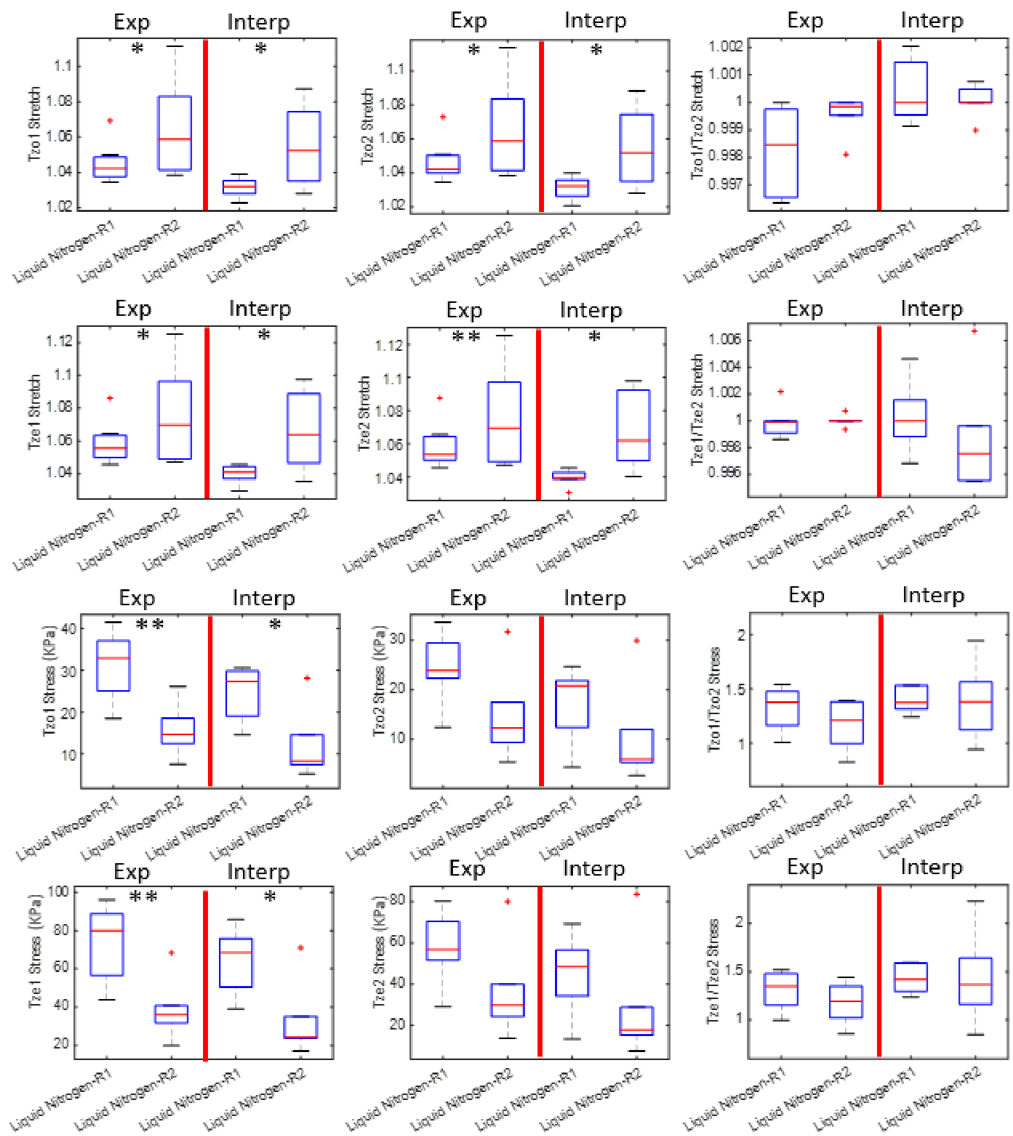


Figure 5.7: Stretches and stresses effective mechanical properties for samples frozen in Liquid Nitrogen

smaller than the same stretches in the sample group further away from the spine[††]. As

[††] "Exp": TZo1-Stretch with $p = 0.016$, TZo2-Stretch with $p = 0.011$, TZe1-Stretch and TZe2-Stretch with $p = 0.005$; "Interp": TZo1-Stretch and TZo2-Stretch with $p = 0.011$, TZe1-Stretch and TZe2-Stretch with $p = 0.01$

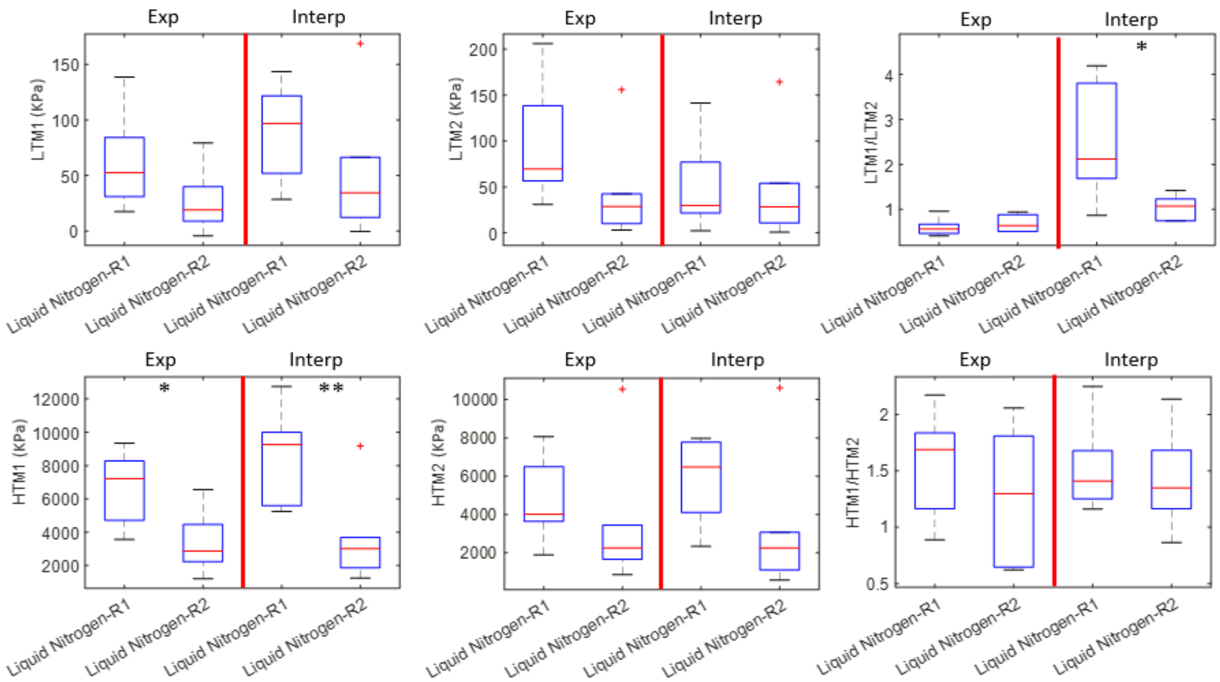


Figure 5.8: Stiffness effective mechanical properties for samples frozen in Liquid Nitrogen

for anisotropy, the ratios did not show any significant differences for both the "Exp" and "Interp" types of analysis. Furthermore, the properties appeared to be more isotropic in most cases. However, TZo1-Stretch, TZo2-Stretch and TZe1-Stretch all appeared to be stiffer for the data extracted using the conventional approach ("Exp"), while TZo2-Stretch and TZe2 were the stiffest for the data extracted using the "Interp" type of analysis.

Next, the stresses associated with the transition zone also revealed significant dependence on the anatomic location in the direction "11" with statistical difference showing smaller p-values for "Exp" type of analysis[‡‡]. Overall, higher stresses were observed in both directions for specimens closer to the spine ("R1"). Notably, the anisotropy results were fairly consistent with no significant differences. TZo1-Stress and TZe1-Stress appeared to

[‡‡] "Exp": TZo1-Stress with $p = 0.0027$, TZe1-Stress with $p = 0.005$; "Interp": TZo1-Stress with $p = 0.02$ and TZe1-Stress with $p = 0.015$

be larger than TZo2-Stress and TZe2-Stress in both zones for both types of analysis.

Finally, figure 5.6 shows the effective mechanical properties associated with stiffness by comparing the Liquid Nitrogen samples located in the "R1" zone to the samples located in the "R2" zone. LTM1 and LTM2 did not reveal any significant differences. Still, both showed, qualitatively, a decrease in the median values for the stiffnesses further away from the spine ("R2") extracted using the "Exp" type of analysis. Similar results were observed for LTM1 from the "Interp" type of analysis, while for LTM2 the median values were matching for both locations. Next, significant differences w.r.t location were deteced for the high tangent modulus in direction "11" (HTM1) in both the conventional ("Exp") and advanced approach ("Interp") ("Exp": HTM1 with $p = 0.014$; "Interp": HTM2 with $p = 0.008$), while for HTM2 no significant differences were revealed. Strikingly, both high tangent moduli of the data extracted using the two types of analysis measured, qualitatively, higher median values for the samples located closer to the spine - "R1". As for anisotropy, only LTM1/LTM2 extracted using the "Interp" type of analysis revealed a significant difference ($p = 0.015$) with samples in "R1" being much stiffer in direction "11". It is interesting to see that, based on the ratio of the tangent moduli extracted using the "Exp" type of analysis, LTM2 was stiffer than LTM1 in both locations (R1 and R2). For high tangent moduli, direction "11" appears to be stiffer on average with matching median values of stiffness for the "Interp" type of analysis and stiffer "R1" samples for the "Exp" type of analysis.

## 5.4 Discussion

In this section, the results obtained from the comparison of the effective mechanical properties of human skin specimens from different locations on the back and stored using different freezing protocols will be discussed.

First, the results of this chapter reflected the results in Chapter 4, where the type of analysis ("Interp" vs "Exp") had noticeable effects on the statistical outcomes. In our simulations, in particular, the statistical difference between groups was diminished in two cases (TZ Stresses in "22" direction) and revealed in one case (HTM1) when "Interp" type of analysis was employed. Interestingly, in Chapter 4, different aortic tissue groups were compared while here we compared different sample groups within the same patients. Therefore, the data extraction approach matters whether it is of interest to detect either inter-group differences (differences between different groups) or intra-patient differences (differences within the same patient). Some studies [1] claim that intra-patient differences may be blurred by inter-patient differences when the combined impact is considered. The robust analysis based on the measures extracted at equivalent deformation states has the potential to make the outcome of statistical studies mixing/separating inter- and intra-effects more reliable.

The comparison of freezing protocols (PBS, Glycerol and Liquid Nitrogen) on the effective mechanical properties of human skin revealed interesting findings. Quantitively, almost no significant differences were detected. The onset and end transition zone stretches were similar for all types of freeze-storage. For instance, in most cases, the median stretches were slightly higher for the Glycerol group compared to PBS and liquid nitrogen groups. However, these qualitative differences were relatively small. Since the transition zone stretches reflect the behaviour of the collagen fibres (see Chapter 1, section 1.1), we can conclude that the configuration of collagen fibres [10] is either relatively unaffected by the way the tissue is stored or affected in the same way for all the freezing protocols. Stiffness LTM associated with elastic fibres and ground substance response at small deformation was also relatively unaffected. However, when considering transition stresses and high-strain tangent moduli HTM, the freezing protocol influenced the mechanical properties to some extent. Because both sets of effective mechanical properties describe the ability of collagen to resist loading, this might indicate that collagen fibres' quality changed depending on the freezing-storage approach. Particularly, the PBS and Glycerol groups were displaying more or less similar results while the Liquid Nitrogen group was more distinct with larger variability detected. This is perhaps not surprising considering that Glycerol solution is mixed with PBS, and thus, both freezing groups create a wet environment for samples to freeze in. Some studies pointed out that the use of Glycerol as a cryopreservation technique is better than PBS [123, 124], but we did not capture any biomechanical differences. Liquid Nitrogen specimens, in contrast, are rapidly freeze-dried and could result in the creation of ice crystals that had a more pronounced impact on the load-bearing capacity of collagen fibres while keeping their configuration (waviness) unaffected [125]. However, it is important to note that these are only qualitative observations and deeper analysis is needed to make a conclusion about specific freezing protocols.

The investigation of heterogeneity along the back provided valuable insights into how effective mechanical properties vary at different locations. Variability based on the location along the back, from the top to the bottom, parallel to the spine, was fairly noticeable in line plots although it is hard to draw any specific conclusion because the statistical analysis could not be performed. Still, some interesting points can be raised. The orientation of collagen fibres is known for the human back based on the maps of Langer lines [72, 127], it is at an angle toward the spine. Because the loading was applied along the spine and perpendicular to the spine, the properties should either exhibit isotropy meaning that fibres are at 45 degrees or anisotropy with a more pronounced response in the direction to which fibres are closer inclined. Based on stresses and stiffnesses, larger stresses are produced in the direction "11" during the collagen recruitment process and the overall stiffness is larger which indicates that fibres are oriented at an angle closer to the perpendicular to the spine. Similar results were observed in [128] for uniaxially tested skin taken from the porcine back pointing out similarities between animal and human back skin models [129]. Notably, there is some variation in values along the back indicating that the preferred orientation and likely dispersion of collagen fibres slightly varies parallel to the spine. Interestingly, transition stretches did not exhibit the tendency to engage earlier in one direction over the other (at least for a more robust "Interp" type of analysis). This might point out the fact that collagen waviness is quite location-dependent with the location-specific functions and underlying microstructure dictating the response, as it was also noted in [46] for equine skin.

The differences between specimens taken closer to the spine and further away from the spine were striking. Based on the transition zone analysis, collagen fibres engaged consistently later for specimens further away from the spine and at, usually, lower stresses (significance was detected for the Liquid Nitrogen group). Stiffness was also mostly lower for the specimens further away from the spine. This points out very different configurations and load-bearing capacities of collagen fibres based on their distance from the spine. Meanwhile, no consistent results were observed for anisotropy, possibly supported by the fact that Langer lines do not experience sudden orientation changes when moving away from the back [127,130].

## 5.5 Limitations

There were some limitations associated with biaxial testing of human back skin samples and biaxial data analysis. First, it was of interest to assess the effect of freezing by comparing freshly tested samples to the frozen specimens studied in this chapter. However, due to some delays in the approval to provide the donor's back samples, as well as some technical issues faced with the biaxial machine, the biaxial testing of fresh samples could not be performed on time. So the designated specimens were used for pilot testing. Second, some samples failed due to issues with image tracking - 3 PBS samples, 2 glycerol samples and 1 liquid nitrogen sample. Because of limited samples in each of the freezing groups, some statistical outcomes could be affected, for instance, the heterogeneity analysis (e.g. Liquid Nitrogen group: 7 vs 6 samples were used in "R1" and "R2" anatomic locations, respectively). Therefore, due to the limited number of PBS samples used on the left side ( in "L1" and "L2") compared to the right side (for Glycerol and Liquid Nitrogen), assessing the symmetry based on the anatomic location would lead to inaccurate results. Next, only tissues from one senior donor have been used in the analysis. More donors need to be used in future studies to confirm/strengthen the results. Finally, the use of quantitative statistics would be a better approach instead of qualitative observations to discuss some of the results, but unfortunately, in most cases, we were limited by the number of samples and the experiment design where the heterogeneity and freezing effects could not be separated Ideally, two different studies have to be conducted in the future where effects of freezing storage and heterogeneity are studied separately.

# Chapter 6

# Significance and Future Work

Mechanical characterization is of high importance in investigating the behaviour of soft biological tissues. Planar biaxial testing is the state-of-the-art test to establish this characterization by capturing the anisotropy and nonlinearity of soft tissues. Biaxial testing is often used to compare effective mechanical properties between different tissue groups and point out important differences. However, the way these effective mechanical properties are extracted is not well discussed across biaxial studies, and most studies choose to extract measures at the inconsistent deformation states that can mislead the statistics.

In this thesis, we proposed a robust approach for the extraction of data from biaxially tested soft biological tissues. This method consists of surface fitting software facilitating the extraction of the effective mechanical properties of soft tissues at the equivalent deformation states. Using real experimental data on the aorta and skin, we were the first to show how the data extraction approach can statistically impact tissue properties and tissue group comparisons' outcomes. Perhaps, future studies should focus on the computational proof-of-concept, in which the finite model of biaxially tested specimens with different fibres' configurations are simulated, and the effective mechanical properties from two set deformation states are extracted and compared.

Using the proposed approach for the data extraction, we were able to point out interesting differences between different aortic tissue groups highlighting how aneurysmal human tissues are microstructurally different from healthy porcine tissues. Future studies should focus on the robust comparison between healthy and pathology-affected aortic tissues to draw conclusions on how microstructure is different between animal and human models and how microstructure is affected by the pathology progression. Extracting the data at the equivalent deformation states, as proposed in our study, will improve the quality of such comparisons.

Next, the proposed approach allowed us to conduct some intra-patient analysis on the human donor back, which, as we argued, could be more affected by the quality of the data extraction approach compared to the inter-tissue type studies. We compared the effect of three freezing solutions on the mechanical properties of the skin - PBS, Glycerol-based PBS and Liquid Nitrogen. Even though we were not able to compare how freezing impact changes the mechanical properties of the fresh tissues, we qualitatively observed that mixing Glycerol with PBS or just using PBS alone does not seem to impact the mechanical properties, while rapid dry-freezing of samples with Liquid Nitrogen leads to some noticeable collagen changes compared with wet-environment freezing of PBS groups. More research should be conducted to conclude which freezing approach is the most suitable, and perhaps, the animal models should be used first due to the difficulties of obtaining fresh human skin. This could improve standards of tissue storage which could be important for many biomedical engineering skin research studies as well as for skin tissue banks and the skin transplantation sector.

Finally, the proposed approach also allowed to study human back skin heterogeneity, even in the context of one patient only. The skin on the back is indeed heterogeneous. Some variability in the skin biomechanics was qualitatively observed along the back parallel to the spine that could be related to the underlying microstructure but no statistical comparisons could be performed. Ideally, the heterogeneity along the back should be studied for a group of patients, which future studies should focus on. Still, some statistically significant changes were observed for samples grouped based on the distance from the spine pointing out remarkable differences in collagen configuration and collagen load-bearing capacity.

This suggests that various studies should be careful when utilizing skin from adjacent locations on the back and treating these samples as equivalent. More research needs to be done to shed light on the reasons behind back skin heterogeneity as back skin is often used in tissue banks.

To re-iterate, this thesis aimed to propose a robust approach of biaxial data extraction from tissues' equivalent deformation states rather than the deformation states that vary from sample to sample. By comparing the conventional and proposed advanced data extraction techniques, we demonstrated how the choice of analysis can impact the extracted mechanical properties in soft tissues and the outcome of the biaxial studies. Furthermore, the investigation into the inter-aortic tissue types differences and the effects of freezing storage protocols/heterogeneity on intra-patient back skin biomechanics emphasized the importance of accurate data extraction. Our findings shed light on the complexities and intricacies involved in characterizing soft tissues, and the implications of these variations on biomechanical studies. Ultimately, this work contributes to advancing the field of mechanical characterization of soft biological tissues and provides a solid foundation for further research in this area, with potential applications in clinical and tissue engineering settings. So after all of that, will future studies consider the importance of data extraction at equivalent deformation states?

# References


[1] Taisiya Sigaeva, Samaneh Sattari, Stanislav Polzer, Jehangir J Appoo, and Elena S Di Martino. Biomechanical properties of ascending aortic aneurysms: quantification of inter-and intra-patient variability. *Journal of Biomechanics*, 125:110542, 2021.

[2] Yuan-cheng Fung. *Biomechanics: mechanical properties of living tissues*. Springer Science & Business Media, 2013.

[3] Isidore Gersh and Hubert R Catchpole. The nature of ground substance of connective tissue. *Perspectives in Biology and Medicine*, 3(2):282–319, 1960.

[4] IHM Muir. The chemistry of the ground substance of joint cartilage. In *The joints and synovial fluid*, pages 27–94. Elsevier, 1980.

[5] John Gosline, Margo Lillie, Emily Carrington, Paul Guerette, Christine Ortlepp, and Ken Savage. Elastic proteins: biological roles and mechanical properties. *Philosophical Transactions of the Royal Society of London. Series B: Biological Sciences*, 357(1418):121–132, 2002.

[6] Austin J Cocciolone, Jie Z Hawes, Marius C Staiculescu, Elizabeth O Johnson, Monzur Murshed, and Jessica E Wagenseil. Elastin, arterial mechanics, and cardiovascular disease. *American Journal of Physiology-Heart and Circulatory Physiology*, 315(2):H189–H205, 2018.

[7] JD Humphrey and FC Yin. A new constitutive formulation for characterizing the mechanical behavior of soft tissues. *Biophysical journal*, 52(4):563–570, 1987.

[8] Wen Yang, Vincent R Sherman, Bernd Gludovatz, Eric Schaible, Polite Stewart, Robert O Ritchie, and Marc A Meyers. On the tear resistance of skin. *Nature communications*, 6(1):1–10, 2015.

[9] Sterling Nesbitt, Wentzell Scott, James Macione, and Shiva Kotha. Collagen fibrils in skin orient in the direction of applied uniaxial load in proportion to stress while exhibiting differential strains around hair follicles. *Materials*, 8(4):1841–1857, 2015.

[10] Gerhard A Holzapfel. Collagen in arterial walls: biomechanical aspects. In *Collagen: structure and mechanics*, pages 285–324. Springer, 2008.

[11] Matthew D Shoulders and Ronald T Raines. Collagen structure and stability. *Annual review of biochemistry*, 78:929–958, 2009.

[12] Alfonso Gautieri, Simone Vesentini, Alberto Redaelli, and Markus J Buehler. Hierarchical structure and nanomechanics of collagen microfibrils from the atomistic scale up. *Nano letters*, 11(2):757–766, 2011.

[13] Cheng-Lun Tsai, Ji-Chung Chen, Wen-Jwu Wang, et al. Near-infrared absorption property of biological soft tissue constituents. *Journal of Medical and Biological Engineering*, 21(1):7–14, 2001.

[14] Yu Zou and Yanhang Zhang. An experimental and theoretical study on the anisotropy of elastin network. *Annals of biomedical engineering*, 37:1572–1583, 2009.

[15] Jérémy Bercoff, Mickael Tanter, and Mathias Fink. Supersonic shear imaging: a new technique for soft tissue elasticity mapping. *IEEE transactions on ultrasonics, ferroelectrics, and frequency control*, 51(4):396–409, 2004.

[16] Mark L Palmeri and Kathryn R Nightingale. Acoustic radiation force-based elasticity imaging methods. *Interface focus*, 1(4):553–564, 2011.

[17] DA Shcherbakova, Clément Papadacci, Abigail Swillens, Annette Caenen, Sander De Bock, Veronique Saey, Koen Chiers, Mickaël Tanter, SE Greenwald, Mathieu Pernot, et al. Supersonic shear wave imaging to assess arterial nonlinear behavior and anisotropy: proof of principle via ex vivo testing of the horse aorta. *Advances in Mechanical Engineering*, 6:272586, 2014.

[18] Yang Sun, Chuan Ma, XiaoLong Liang, Run Wang, Ying Fu, ShuMin Wang, LiGang Cui, and ChunLei Zhang. Reproducibility analysis on shear wave elastography (swe)-based quantitative assessment for skin elasticity. *Medicine*, 96(19), 2017.

[19] Pauline Zamprogno, Giuditta Thoma, Veronika Cencen, Dario Ferrari, Barbara Putz, Johann Michler, Georg E Fantner, and Olivier T Guenat. Mechanical properties of soft biological membranes for organ-on-a-chip assessed by bulge test and afm. *ACS biomaterials science & engineering*, 7(7):2990–2997, 2021.

[20] Tammy L Haut Donahue, ML Hull, Mark M Rashid, and Christopher R Jacobs. A finite element model of the human knee joint for the study of tibio-femoral contact. *J. Biomech. Eng.*, 124(3):273–280, 2002.

[21] Van C Mow, Anthony Ratcliffe, and A Robin Poole. Cartilage and diarthrodial joints as paradigms for hierarchical materials and structures. *Biomaterials*, 13(2):67–97, 1992.

[22] RM Delaine-Smith, S Burney, FR Balkwill, and MM Knight. Experimental validation of a flat punch indentation methodology calibrated against unconfined compression tests for determination of soft tissue biomechanics. *Journal of the mechanical behavior of biomedical materials*, 60:401–415, 2016.

[23] Kristy B Arbogast, Kirk L Thibault, B Scott Pinheiro, Karen I Winey, and Susan S Margulies. A high-frequency shear device for testing soft biological tissues. *Journal of biomechanics*, 30(7):757–759, 1997.

[24] Ivan Argatov and Gennady Mishuris. *Indentation testing of biological materials*, volume 91. Springer, 2018.

[25] Javier Palacio-Torralba, Steven Hammer, Daniel W Good, S Alan McNeill, Grant D Stewart, Robert L Reuben, and Yuhang Chen. Quantitative diagnostics of soft tissue through viscoelastic characterization using time-based instrumented palpation. *journal of the mechanical behavior of biomedical materials*, 41:149–160, 2015.

[26] Spencer P Lake, Kristin S Miller, Dawn M Elliott, and Louis J Soslowsky. Effect of fiber distribution and realignment on the nonlinear and inhomogeneous mechanical properties of human supraspinatus tendon under longitudinal tensile loading. *Journal of Orthopaedic Research*, 27(12):1596–1602, 2009.

[27] Michael S Sacks and Wei Sun. Multiaxial mechanical behavior of biological materials. *Annual review of biomedical engineering*, 5(1):251–284, 2003.

[28] JE Field, SM Walley, NK Bourne, and JM Huntley. Experimental methods at high rates of strain. *Le Journal de Physique IV*, 4(C8):C8–3, 1994.

[29] G Gerard and R Papirno. Dynamic biaxial stress-strain characteristics of aluminum and mild steel. *Trans. Amer. Soc. Metals*, 49:132–148, 1957.

[30] Y Lanir and YC Fung. Two-dimensional mechanical properties of rabbit skin—i. experimental system. *Journal of Biomechanics*, 7(1):29–34, 1974.

[31] Dorel Banabic, Frédéric Barlat, Oana Cazacu, and Toshihiko Kuwabara. Advances in anisotropy and formability. *International journal of material forming*, 3:165–189, 2010.

[32] Nathan T Jacobs, Daniel H Cortes, Edward J Vresilovic, and Dawn M Elliott. Biaxial tension of fibrous tissue: using finite element methods to address experimental challenges arising from boundary conditions and anisotropy. *Journal of biomechanical engineering*, 135(2), 2013.

[33] Todd Courtney, Michael S Sacks, John Stankus, Jianjun Guan, and William R Wagner. Design and analysis of tissue engineering scaffolds that mimic soft tissue mechanical anisotropy. *Biomaterials*, 27(19):3631–3638, 2006.

[34] Yan Lanir. Constitutive equations for fibrous connective tissues. *Journal of biomechanics*, 16(1):1–12, 1983.

[35] Walter Maurel, Daniel Thalmann, Yin Wu, and Nadia Magnenat Thalmann. *Biomechanical models for soft tissue simulation*, volume 48. Springer, 1998.

[36] Samaneh Sattari, Crystal A Mariano, and Mona Eskandari. Biaxial mechanical properties of the bronchial tree: Characterization of elasticity, extensibility, and energetics, including the effect of strain rate and preconditioning. *Acta Biomaterialia*, 155:410–422, 2023.

[37] Miriam Nightingale, Alexander Gregory, Taisiya Sigaeva, Gary M. Dobson, Paul W.M. Fedak, Jehangir J. Appoo, Elena S. Di Martino, Miriam Nightingale, Alexander Gregory, Richard Beddoes, Alicia Nickel, Samaneh Sattari, Taisiya Sigaeva, Amy Bromley, Jehangir J. Appoo, and Elena S. Di Martino. Biomechanics in ascending aortic aneurysms correlate with tissue composition and strength. *JTCVS Open*, 9:1–10, 2022.

[38] MS Sacks. A method for planar biaxial mechanical testing that includes in-plane shear. 1999.

[39] Michael S Sacks. Biaxial mechanical evaluation of planar biological materials. *Journal of elasticity and the physical science of solids*, 61:199–246, 2000.

[40] Michael S Sacks and CJ Chuong. Orthotropic mechanical properties of chemically treated bovine pericardium. *Annals of biomedical engineering*, 26:892–902, 1998.

[41] Jonathan P Vande Geest, Michael S Sacks, and David A Vorp. The effects of aneurysm on the biaxial mechanical behavior of human abdominal aorta. *Journal of biomechanics*, 39(7):1324–1334, 2006.

[42] Devin Laurence, Colton Ross, Samuel Jett, Cortland Johns, Allyson Echols, Ryan Baumwart, Rheal Towner, Jun Liao, Pietro Bajona, Yi Wu, et al. An investigation of regional variations in the biaxial mechanical properties and stress relaxation behaviors of porcine atrioventricular heart valve leaflets. *Journal of biomechanics*, 83:16–27, 2019.

[43] Takeo Matsumoto, Tomohiro Fukui, Toshihiro Tanaka, Naoko Ikuta, Toshiro Ohashi, Kiichiro Kumagai, Hiroji Akimoto, Koichi Tabayashi, and Masaaki Sato. Biaxial tensile properties of thoracic aortic aneurysm tissues. *Journal of Biomechanical Science and Engineering*, 4(4):518–529, 2009.

[44] Reza Avazmohammadi, Michael R Hill, Marc A Simon, Will Zhang, and Michael S Sacks. A novel constitutive model for passive right ventricular myocardium: evidence for myofiber–collagen fiber mechanical coupling. *Biomechanics and modeling in mechanobiology*, 16:561–581, 2017.

[45] Michael S Sacks, Will Zhang, and Silvia Wognum. A novel fibre-ensemble level constitutive model for exogenous cross-linked collagenous tissues. *Interface focus*, 6(1):20150090, 2016.

[46] Holly D Sparks, Taisiya Sigaeva, Samar Tarraf, Serena Mandla, Hannah Pope, Olivia Hee, Elena S Di Martino, Jeff Biernaskie, Milica Radisic, and W Michael Scott. Biomechanics of wound healing in an equine limb model: effect of location and treatment with a peptide-modified collagen–chitosan hydrogel. *ACS Biomaterials Science & Engineering*, 7(1):265–278, 2020.

[47] David B Smith, Michael S Sacks, David A Vorp, and Michael Thornton. Surface geometric analysis of anatomic structures using biquintic finite element interpolation. *Annals of biomedical engineering*, 28:598–611, 2000.

[48] Ghassan S Kassab. Biomechanics of the cardiovascular system: the aorta as an illustratory example. *Journal of the Royal Society Interface*, 3(11):719–740, 2006.

[49] William C Aird. Phenotypic heterogeneity of the endothelium: Ii. representative vascular beds. *Circulation research*, 100(2):174–190, 2007.

[50] Ludwig K von Segesser, Igor Killer, Marcel Ziswiler, Andre Linka, Manfred Ritter, Rolf Jenni, Peter C Baumann, and Marko I Turina. Dissection of the descending thoracic aorta extending into the ascending aorta: a therapeutic challenge. *The Journal of Thoracic and Cardiovascular Surgery*, 108(4):755–761, 1994.

[51] Gustav G Belz. Elastic properties and windkessel function of the human aorta. *Cardiovascular drugs and therapy*, 9:73–83, 1995.

[52] Sheldon Weinbaum, John M Tarbell, and Edward R Damiano. The structure and function of the endothelial glycocalyx layer. *Annu. Rev. Biomed. Eng.*, 9:121–167, 2007.

[53] Furqan A Rajput and Roman Zeltser. Aortic valve replacement. 2019.

[54] Natzi Sakalihasan, Raymond Limet, and Olivier Damien Defawe. Abdominal aortic aneurysm. *The Lancet*, 365(9470):1577–1589, 2005.

[55] Elliot L Chaikof, Ronald L Dalman, Mark K Eskandari, Benjamin M Jackson, W Anthony Lee, M Ashraf Mansour, Tara M Mastracci, Matthew Mell, M Hassan Murad, Louis L Nguyen, et al. The society for vascular surgery practice guidelines on the care of patients with an abdominal aortic aneurysm. *Journal of vascular surgery*, 67(1):2–77, 2018.

[56] Jonathan Golledge and Paul E Norman. Current status of medical management for abdominal aortic aneurysm. *Atherosclerosis*, 217(1):57–63, 2011.

[57] Barry T Katzen, Michael D Dake, Alexandra A MacLean, and David S Wang. Endovascular repair of abdominal and thoracic aortic aneurysms. *Circulation*, 112(11):1663–1675, 2005.

[58] Hector I Michelena, Alessandro Della Corte, Siddharth K Prakash, Dianna M Milewicz, Artur Evangelista, and Maurice Enriquez-Sarano. Bicuspid aortic valve aortopathy in adults: incidence, etiology, and clinical significance. *International journal of cardiology*, 201:400–407, 2015.

[59] Majid Jadidi, Mahmoud Habibnezhad, Eric Anttila, Kaspars Maleckis, Anastasia Desyatova, Jason MacTaggart, and Alexey Kamenskiy. Mechanical and structural changes in human thoracic aortas with age. *Acta biomaterialia*, 103:172–188, 2020.

[60] Gerhard A Holzapfel, Thomas C Gasser, and Ray W Ogden. A new constitutive framework for arterial wall mechanics and a comparative study of material models. *Journal of elasticity and the physical science of solids*, 61:1–48, 2000.

[61] Alexey V Kamenskiy, Yuris A Dzenis, Syed A Jaffar Kazmi, Mark A Pemberton, Iraklis I Pipinos, Nick Y Phillips, Kyle Herber, Thomas Woodford, Robert E Bowen, Carol S Lomneth, et al. Biaxial mechanical properties of the human thoracic and abdominal aorta, common carotid, subclavian, renal and common iliac arteries. *Biomechanics and modeling in mechanobiology*, 13(6):1341–1359, 2014.

[62] Siobhan A O'Leary, Donagh A Healey, Eamon G Kavanagh, Michael T Walsh, Tim M McGloughlin, and Barry J Doyle. The biaxial biomechanical behavior of abdominal aortic aneurysm tissue. *Annals of biomedical engineering*, 42:2440–2450, 2014.

[63] Russell O Potts and Michael L Francoeur. Lipid biophysics of water loss through the skin. *Proceedings of the National Academy of Sciences*, 87(10):3871–3873, 1990.

[64] Ethan R Nadel, Robert W Bullard, and JA Stolwijk. Importance of skin temperature in the regulation of sweating. *Journal of applied physiology*, 31(1):80–87, 1971.

[65] Wedad Z Mostafa and Rehab A Hegazy. Vitamin d and the skin: Focus on a complex relationship: A review. *Journal of advanced research*, 6(6):793–804, 2015.

[66] Oliver Alexander Shergold. *The mechanics of needle-free injection.* PhD thesis, University of Cambridge, 2004.

[67] H Eshel and Y Lanir. Effects of strain level and proteoglycan depletion on preconditioning and viscoelastic responses of rat dorsal skin. *Annals of Biomedical Engineering*, 29:164–172, 2001.

[68] P Agache. Physiology of the skin and cutaneous functional explorations, collection explorations fonctionnelles humaines. *Editions Médicales Internationales. France: Cachan*, 2000.

[69] Fouad Khatyr, Claude Imberdis, Paul Vescovo, Daniel Varchon, and Jean-Michel Lagarde. Model of the viscoelastic behaviour of skin in vivo and study of anisotropy. *Skin research and technology*, 10(2):96–103, 2004.

[70] Alireza Karimi, Maedeh Haghighatnama, Ahmad Shojaei, Mahdi Navidbakhsh, Afsaneh Motevalli Haghi, and Seyed Jafar Adnani Sadati. Measurement of the viscoelastic mechanical properties of the skin tissue under uniaxial loading. *Proceedings of the Institution of Mechanical Engineers, Part L: Journal of Materials: Design and Applications*, 230(2):418–425, 2016.

[71] Andrei Pissarenko and Marc A Meyers. The materials science of skin: Analysis, characterization, and modeling. *Progress in Materials Science*, 110:100634, 2020.

[72] Karl Langer. On the anatomy and physiology of the skin. *British journal of plastic surgery*, 31(1):3–8, 1978.

[73] Michael H Flint. The biological basis of langer's lines. *The ultrastructure of collagen*, pages 132–140, 1976.

[74] Peter Grant Martin. *Properties of human skin*. University of Virginia, 2000.

[75] Simon P DiMaio and Septimiu E Salcudean. Needle insertion modeling and simulation. *IEEE Transactions on robotics and automation*, 19(5):864–875, 2003.

[76] Simon P DiMaio and Septimiu E Salcudean. Interactive simulation of needle insertion models. *IEEE transactions on biomedical engineering*, 52(7):1167–1179, 2005.

[77] Niki Abolhassani, Rajni Patel, and Mehrdad Moallem. Needle insertion into soft tissue: A survey. *Medical engineering & physics*, 29(4):413–431, 2007.

[78] Rostislav V Shevchenko, Stuart L James, and S Elizabeth James. A review of tissue-engineered skin bioconstructs available for skin reconstruction. *Journal of the royal Society Interface*, 7(43):229–258, 2010.

[79] Jessica WY Jor, Matthew D Parker, Andrew J Taberner, Martyn P Nash, and Poul MF Nielsen. Computational and experimental characterization of skin mechanics: identifying current challenges and future directions. *Wiley Interdisciplinary Reviews: Systems Biology and Medicine*, 5(5):539–556, 2013.

[80] Y Lanir and YC Fung. Two-dimensional mechanical properties of rabbit skin—i. experimental system. *Journal of Biomechanics*, 7(1):29–34, 1974.

[81] Dennis C Schneider, Terence M Davidson, and Alan M Nahum. In vitro biaxial stress-strain response of human skin. *Archives of Otolaryngology*, 110(5):329–333, 1984.

[82] GA Holzapfel and RW Ogden. In press. on planar biaxial tests for anisotropic nonlinearly elastic solids: a continuum mechanical framework. *Math. Mech. Solids*.

[83] Gerhard A Holzapfel, Ray W Ogden, and Selda Sherifova. On fibre dispersion modelling of soft biological tissues: a review. *Proceedings of the Royal Society A*, 475(2224):20180736, 2019.

[84] AJ Skulborstad, SM Swartz, and NC Goulbourne. Biaxial mechanical characterization of bat wing skin. *Bioinspiration & Biomimetics*, 10(3):036004, 2015.

[85] Jessica E Wagenseil and Robert P Mecham. Vascular extracellular matrix and arterial mechanics. *Physiological reviews*, 89(3):957–989, 2009.

[86] Zbyněk Tonar, Tereza Kubíková, Claudia Prior, Erna Demjén, Václav Liška, Milena Králíčková, and Kirsti Witter. Segmental and age differences in the elastin network,

collagen, and smooth muscle phenotype in the tunica media of the porcine aorta. *Annals of Anatomy-Anatomischer Anzeiger*, 201:79–90, 2015.

[87] Simon Joost, Amit Zeisel, Tina Jacob, Xiaoyan Sun, Gioele La Manno, Peter Lönnerberg, Sten Linnarsson, and Maria Kasper. Single-cell transcriptomics reveals that differentiation and spatial signatures shape epidermal and hair follicle heterogeneity. *Cell systems*, 3(3):221–237, 2016.

[88] Xinhong Lim and Roel Nusse. Wnt signaling in skin development, homeostasis, and disease. *Cold Spring Harbor perspectives in biology*, 5(2):a008029, 2013.

[89] Frank O Nestle, Paola Di Meglio, Jian-Zhong Qin, and Brian J Nickoloff. Skin immune sentinels in health and disease. *Nature Reviews Immunology*, 9(10):679–691, 2009.

[90] Mythily Srinivasan, Daniel Sedmak, and Scott Jewell. Effect of fixatives and tissue processing on the content and integrity of nucleic acids. *The American journal of pathology*, 161(6):1961–1971, 2002.

[91] Hui Xu, Hua Wan, Wenqi Zuo, Wendell Sun, Rick T Owens, John R Harper, David L Ayares, and David J McQuillan. A porcine-derived acellular dermal scaffold that supports soft tissue regeneration: removal of terminal galactose-$\alpha$-(1, 3)-galactose and retention of matrix structure. *Tissue Engineering Part A*, 15(7):1807–1819, 2009.

[92] Ming-Jay Chow and Yanhang Zhang. Changes in the mechanical and biochemical properties of aortic tissue due to cold storage. *Journal of Surgical Research*, 171(2):434–442, 2011.

[93] C Thomas Vangsness JR, Mark J Triffon, Michael J Joyce, and Tillman M Moore. Soft tissue for allograft reconstruction of the human knee: a survey of the american association of tissue banks. *The American journal of sports medicine*, 24(2):230–234, 1996.

[94] CC Bondoc and JF Burke. Clinical experience with viable frozen human skin and a frozen skin bank. *Annals of surgery*, 174(3):371, 1971.

[95] Aimee Schimizzi, Michelle Wedemeyer, Tim Odell, Walter Thomas, Andrew T Mahar, and Robert Pedowitz. Effects of a novel sterilization process on soft tissue mechanical properties for anterior cruciate ligament allografts. *The American Journal of Sports Medicine*, 35(4):612–616, 2007.

[96] SA Ranamukhaarachchi, S Lehnert, SL Ranamukhaarachchi, L Sprenger, T Schneider, I Mansoor, K Rai, UO Häfeli, and B Stoeber. A micromechanical comparison of human and porcine skin before and after preservation by freezing for medical device development. *Scientific reports*, 6(1):1–9, 2016.

[97] Harold T Meryman. Tissue freezing and local cold injury. *Physiological Reviews*, 37(2):233–251, 1957.

[98] Savio L-Y Woo, Carlo A Orlando, Jonathan F Camp, and Wayne H Akeson. Effects of postmortem storage by freezing on ligament tensile behavior. *Journal of biomechanics*, 19(5):399–404, 1986.

[99] Armin Eilaghi, John G Flanagan, G Wayne Brodland, and C Ross Ethier. Strain uniformity in biaxial specimens is highly sensitive to attachment details. 2009.

[100] Heleen Fehervary, Marija Smoljkić, Jos Vander Sloten, and Nele Famaey. Planar biaxial testing of soft biological tissue using rakes: A critical analysis of protocol and fitting process. *Journal of the mechanical behavior of biomedical materials*, 61:135–151, 2016.

[101] Wei Sun, Michael S Sacks, and Michael J Scott. Effects of boundary conditions on the estimation of the planar biaxial mechanical properties of soft tissues. 2005.

[102] YL Dong and Bing Pan. A review of speckle pattern fabrication and assessment for digital image correlation. *Experimental Mechanics*, 57:1161–1181, 2017.

[103] Marco Palanca, Gianluca Tozzi, and Luca Cristofolini. The use of digital image correlation in the biomechanical area: a review. *International biomechanics*, 3(1):1–21, 2016.

[104] Miriam Nightingale, Alexander Gregory, Taisiya Sigaeva, Gary M Dobson, Paul WM Fedak, Jehangir J Appoo, Elena S Di Martino, Richard Beddoes, Alicia Nickel, Samaneh Sattari, et al. Biomechanics in ascending aortic aneurysms correlate with tissue composition and strength. *JTCVS open*, 9:1–10, 2022.

[105] Jianjun Guan, Kazuro L Fujimoto, and William R Wagner. Elastase-sensitive elastomeric scaffolds with variable anisotropy for soft tissue engineering. *Pharmaceutical research*, 25:2400–2412, 2008.

[106] Douglas C Montgomery, Elizabeth A Peck, and G Geoffrey Vining. *Introduction to linear regression analysis*. John Wiley & Sons, 2021.

[107] NR Draper and H Smith. Applied regression analysis. hoboken; somerset, 2014.

[108] Abdul Nurunnabi, Geoff West, and David Belton. Robust locally weighted regression for ground surface extraction in mobile laser scanning 3d data. *ISPRS Annals of the Photogrammetry, Remote Sensing and Spatial Information Sciences*, 2:217–222, 2013.

[109] Richard J Harrison and Joshua M Feinberg. Forcinel: An improved algorithm for calculating first-order reversal curve distributions using locally weighted regression smoothing. *Geochemistry, Geophysics, Geosystems*, 9(5), 2008.

[110] Taisiya Sigaeva, Stanislav Polzer, Radek Vitásek, and Elena S Di Martino. Effect of testing conditions on the mechanical response of aortic tissues from planar biaxial experiments: Loading protocol and specimen side. *Journal of the Mechanical Behavior of Biomedical Materials*, 111:103882, 2020.

[111] Samar A. Tarraf, Benjamin Kramer, Emily Vianna, Callan Gillespie, Emídio Germano, Kelly B. Emerton, Rouzbeh Amini, Robb Colbrunn, Jennifer Hargrave, Eric E.

Roselli, and Chiara Bellini. Lengthwise regional mechanics of the human aneurysmal ascending thoracic aorta. *Acta Biomaterialia*, 162:266–277, 2023.

[112] Hector WL de Beaufort, Anna Ferrara, Michele Conti, Frans L Moll, Joost A van Herwaarden, C Alberto Figueroa, Jean Bismuth, Ferdinando Auricchio, and Santi Trimarchi. Comparative analysis of porcine and human thoracic aortic stiffness. *European Journal of Vascular and Endovascular Surgery*, 55(4):560–566, 2018.

[113] Dinara Zhalmuratova, Thanh-Giang La, Katherine Ting-Ting Yu, Alexander RA Szojka, Stephen HJ Andrews, Adetola B Adesida, Chun-il Kim, David S Nobes, Darren H Freed, and Hyun-Joong Chung. Mimicking "j-shaped" and anisotropic stress–strain behavior of human and porcine aorta by fabric-reinforced elastomer composites. *ACS applied materials & interfaces*, 11(36):33323–33335, 2019.

[114] Linda L Demer and FC Yin. Passive biaxial mechanical properties of isolated canine myocardium. *The Journal of physiology*, 339(1):615–630, 1983.

[115] MC Lee, MARTIN M LeWinter, GREGORY Freeman, RALPH Shabetai, and YC Fung. Biaxial mechanical properties of the pericardium in normal and volume overload dogs. *American Journal of Physiology-Heart and Circulatory Physiology*, 249(2):H222–H230, 1985.

[116] Paul H Chew, Frank CP Yin, and Scott L Zeger. Biaxial stress-strain properties of canine pericardium. *Journal of molecular and cellular cardiology*, 18(6):567–578, 1986.

[117] Raymond P Vito. The mechanical properties of soft tissues—i: A mechanical system for bi-axial testing. *Journal of biomechanics*, 13(11):947–950, 1980.

[118] Grace A Duginski, Colton J Ross, Devin W Laurence, Cortland H Johns, and Chung-Hao Lee. An investigation of the effect of freezing storage on the biaxial mechanical properties of excised porcine tricuspid valve anterior leaflets. *Journal of the mechanical behavior of biomedical materials*, 101:103438, 2020.

[119] Ramji T Venkatasubramanian, Erin D Grassl, Victor H Barocas, Daniel Lafontaine, and John C Bischof. Effects of freezing and cryopreservation on the mechanical properties of arteries. *Annals of Biomedical engineering*, 34:823–832, 2006.

[120] DY Gao, S Lin, PF Watson, and JK Critser. Fracture phenomena in an isotonic salt solution during freezing and their elimination using glycerol. *Cryobiology*, 32(3):270–284, 1995.

[121] Peter Mazur and Kenneth W Cole. Roles of unfrozen fraction, salt concentration, and changes in cell volume in the survival of frozen human erythrocytes. *Cryobiology*, 26(1):1–29, 1989.

[122] Peter Mazur and Robert H. Miller. Survival of frozen-thawed human red cells as a function of the permeation of glycerol and sucrose. *Cryobiology*, 13(5):523–536, 1976.

[123] Lovro Suhodolčan, Miha Brojan, Franc Kosel, Matej Drobnič, Armin Alibegović, and Janez Brecelj. Cryopreservation with glycerol improves the in vitro biomechanical characteristics of human patellar tendon allografts. *Knee Surgery, Sports Traumatology, Arthroscopy*, 21:1218–1225, 2013.

[124] David K Moscatello, Megan Dougherty, Rhoda S Narins, and Naomi Lawrence. Cryopreservation of human fat for soft tissue augmentation: viability requires use of cryoprotectant and controlled freezing and storage. *Dermatologic surgery*, 31:1506–1510, 2005.

[125] Jorge O Virues Delgadillo, Sebastien Delorme, Rouwayda El-Ayoubi, Robert DiRaddo, Savvas G Hatzikiriakos, et al. Effect of freezing on the passive mechanical properties of arterial samples. *Journal of Biomedical Science and Engineering*, 3(07):645, 2010.

[126] Suman Jaiswal, Taisiya Sigaeva, Siva PV Nadimpalli, Samuel Lieber, and Shawn A Chester. Characterization and modeling of the anisotropic behavior of the porcine dermis. *Mechanics Research Communications*, 129:104098, 2023.

[127] Aisling Ní Annaidh and Michel Destrade. Tension lines of the skin. In *Skin Biophysics*, pages 265–280. Springer, 2019.

[128] Oliver A Shergold, Norman A Fleck, and Darren Radford. The uniaxial stress versus strain response of pig skin and silicone rubber at low and high strain rates. *International journal of impact engineering*, 32(9):1384–1402, 2006.

[129] Robert L Bronaugh, Raymond F Stewart, and Elaine R Congdon. Methods for in vitro percutaneous absorption studies ii. animal models for human skin. *Toxicology and applied pharmacology*, 62(3):481–488, 1982.

[130] Wenguang Li. Modelling methods for in vitro biomechanical properties of the skin: a review. *Biomedical Engineering Letters*, 5(4):241–250, 2015.

# APPENDICES

# Appendix A

# Additional Plots Showing the Results for Chapter 5

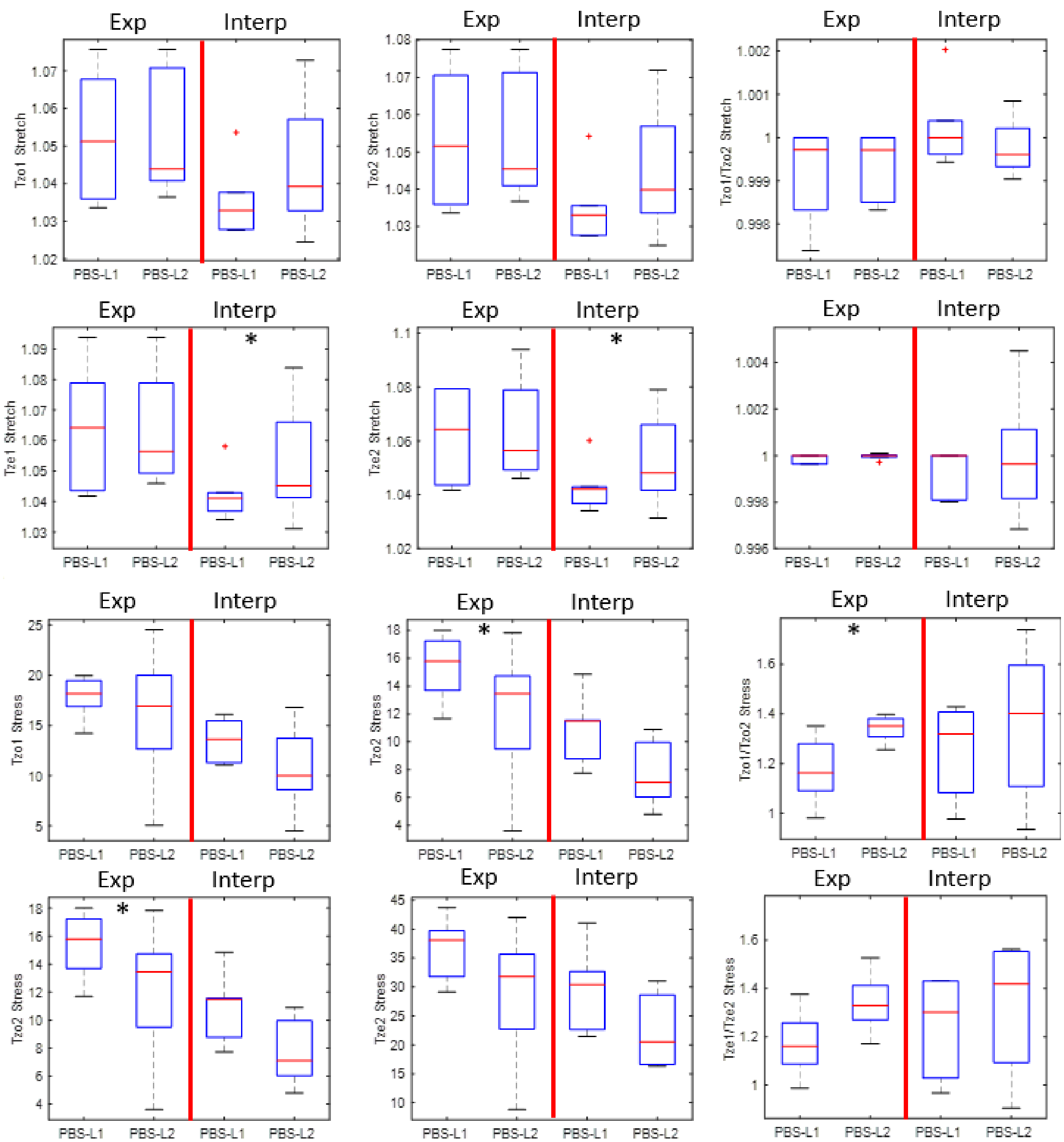


Figure A.1: Stretches and stresses effective mechanical properties for samples frozen in PBS

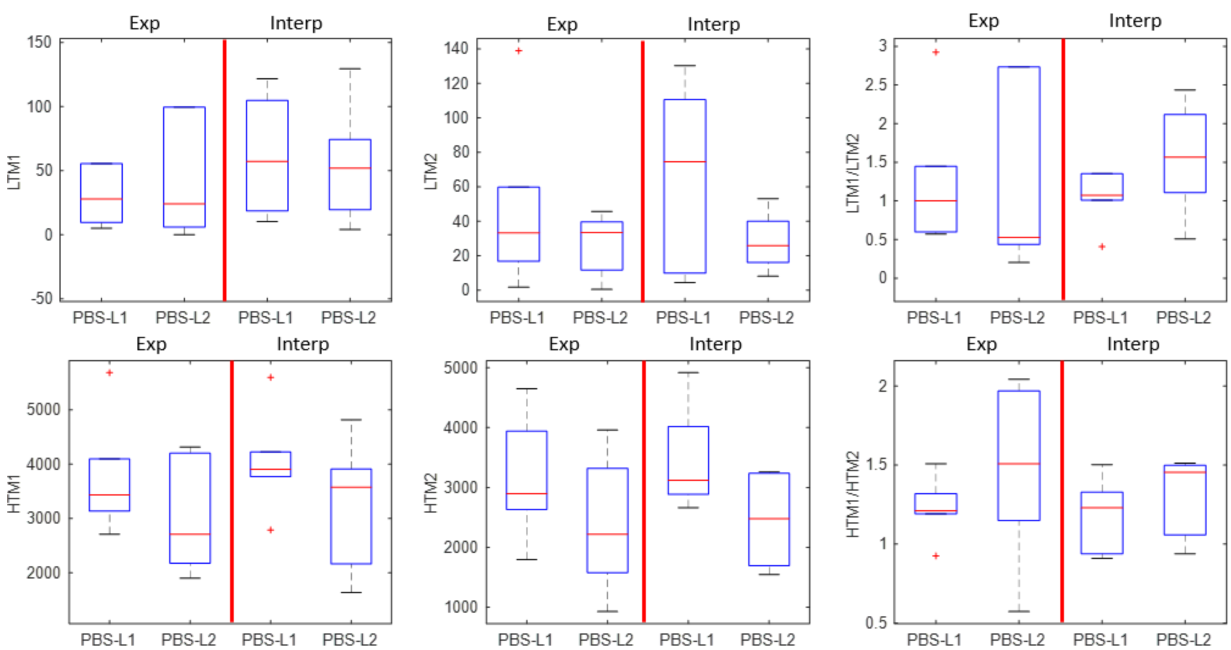


Figure A.2: Stiffness effective mechanical properties for samples frozen in PBS

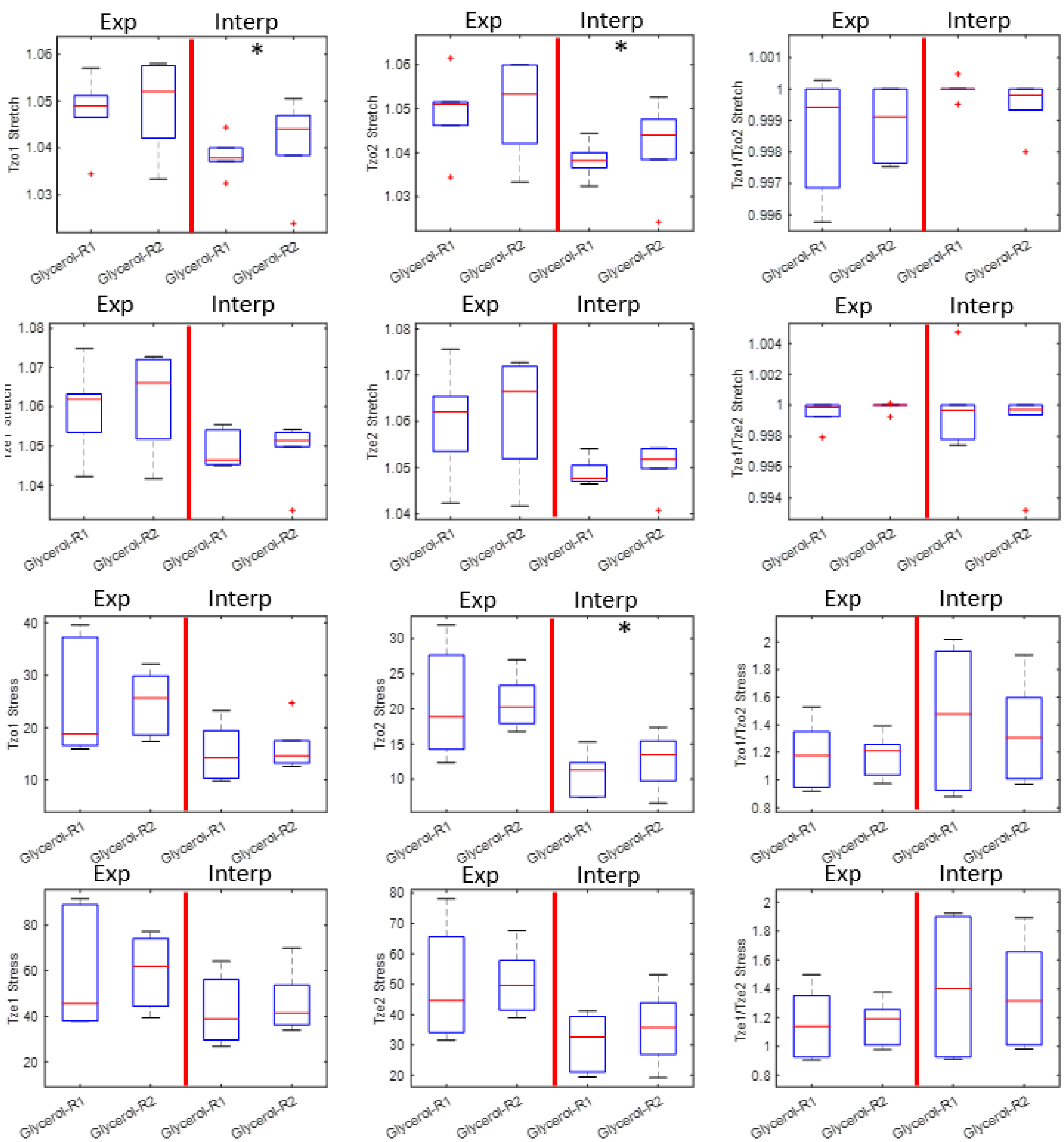


Figure A.3: Stretches and stresses effective mechanical properties for samples frozen in glycerol

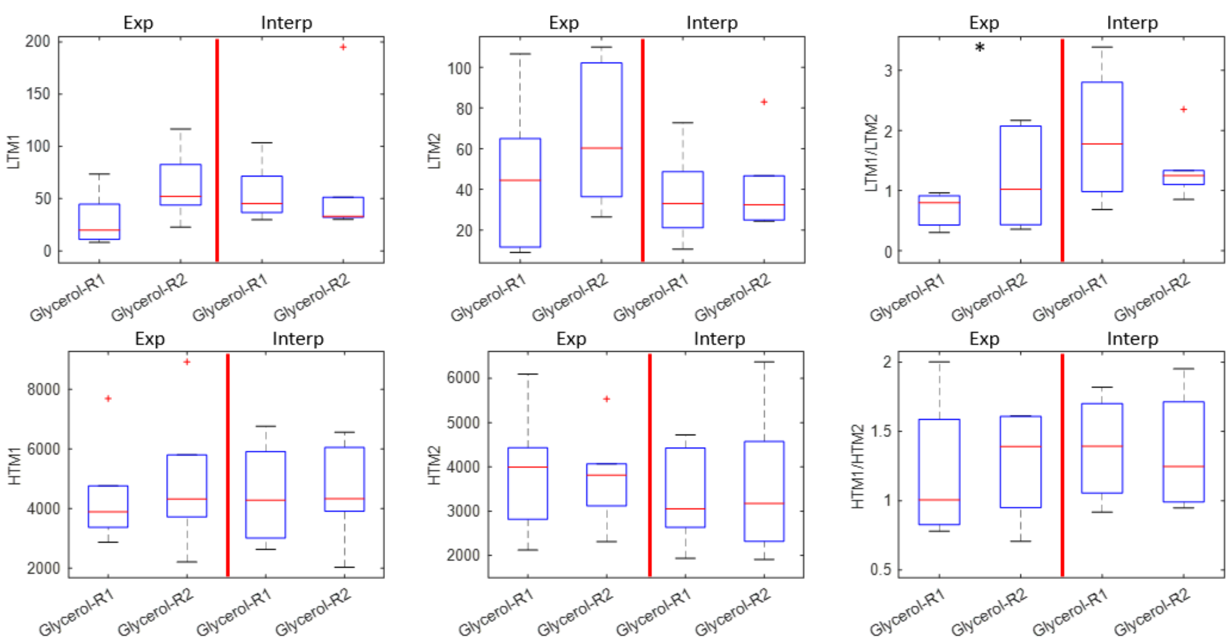


Figure A.4: Stiffness effective mechanical properties for samples frozen in glycerol